# Authors response to reviews
# Turbulence Induced Cloud Voids: Observation and Interpretation

Katarzyna Karpinska[1], Jonathan F.E. Bodenschatz[2], Szymon P. Malinowski[1], Jakub L. Nowak[1], Steffen Risius[2], Tina Schmeissner[4], Raymond A. Shaw[3], Holger Siebert[4], Hengdong Xi[2], Haitao Xu[2], and Eberhard Bodenschatz[2]

[1]Institute of Geophysics, Faculty of Physics, University of Warsaw, Warsaw, Poland
[2]Max Planck Institute for Dynamics and Self-Organization, Goetingen, Germany
[3]Michigan Technological University, Houghton, Michigan, USA
[4]Leibniz Institute for Tropospheric Research, Leipzig, Germany

**Review 1**

This paper describes a theoretical explanation of physical mechanism of generating voids in clouds and some results of kinematic simulation. First, the authors explain the measurements of droplets inside cloud made at the top of German Alps. Then the size distribution of droplets is presented and the voids in the cloud droplet distribution are reported in figures and videos, which are very interesting. Next, the authors study the physical mechanism of void formation. Basic idea is to use the idea that an inertial particle tends to be expelled from the core of Burgers vortex. Theoretical analysis for this physics had already been done by Marqu et al.cited in the reference, and the present paper applies, in its essence, simply the results to the void formation. In order to see whether such interpretation is the case, the authors perform the kinematic simulation, to numerically integrate a set of equations of particles with different sizes in the flow field generated by the Burgers vortex. For two cases of parameters among three cases, the distribution of droplets is found to generate voids, which is consistent with Fig.5 of the theoretical prediction. Finally they argue the physical mechanism from the view points of the present analysis and visualization of voids.

The parts of the experiment and kinematic simulation are, I think, new and it is an idea to use the analysis in terms of Burgers vortex flow to explain the void formation. However, the part regarding the equilibrium positions and their stability is poorly written and hard to follow.

The pages of p. 9-11 use the results of Marqu et al. without definition of some quantities, such as $\varphi$ and $r_0$ . While the authors present the parameter range for stable periodic orbit in Fig.5, the kinematic simulations were done only for three points in the figure. Examination of the relevance of the simulation results by comparing to the theoretical results is not enough to convince the physical reasoning of void formation. Also in the discussion, the authors argue Mie scattering as one possibility of observing the void, but this is a speculation and lacks fundamental data or analysis. In conclusion, the present manuscript needs considerable revision.

**We substantially edited the manuscript, in particular the part regarding the equilibrium positions and their stability**

**with respect to void creation in order to improve presentation quality. We also substantially modified the discussion concerning Mie scattering in order to discuss its effect on the collected data or images in a more clear way.**

Technical points are listed below.

1. p.8, 4th line. the authors write A as the strain parameter. I think, this is not appropriate. $\Gamma$ is the circulation of the Burgers vortex so that $A = 1/Re$ where Re is the Reynolds number of the vortex.
   $A$ **is called "nondimensional strain parameter" in agreement with the name used in the work Marcu et al. (1995). It is true that it is an inverse of vortex Reynolds number and this information was added in the text.**

2. p.9. What are definitions of $r_0$ and $\varphi(r_0)$ ? The paragraph of eqs. (7) and (8) without explanation does not make arguments useful.

   $r_0^*$ **is just the notation for arbitrary solution of the Eq.6. The function** $\varphi(r_0^*)$ **has no parameters. On the basis of this suggestion the text was modified to expressed the intention expicitely.**

3. p.11 How is Acr determined?
   $A_{cr}$ **is defined at p.9. Its value is obtained numerically. For** $A = A_{cr}$ **the equillibrium curve has a horizontal slope at the inflection point.**

**Review 2**

Authors report about an experimental investigation of the behaviour of water droplets measured in cloudy air at a mountain-top station. In particular, they focus on cloud voids, that is spatial regions which are devoid of droplets. To explain the observed phenomenon, they perform a numerical study of a model of inertial particles moving in a Burgers vortex (Marcu et al 1995), under the action of drag and gravity forces. On the basis of these results, with model parameters matched to those of the experiments, authors draw the conclusion that cloud voids observed under the experimental conditions were very likely a result of the presence of relatively thin yet long vortex tubes. The most interesting part of this work is the observation of the phenomenon: cloud voids at the centimetre scale tell us that cloud droplets do not distribute homogeneously in space and that inhomogeneities take place also at scales much larger than the estimated Kolmogorov scale of the flow.

As for the analysis and interpretation of results, I find it weak for the following reasons. To me, the application of a simplified model like the Burgers vortex one is meaningful if we can learn something new about the dynamics of inertial particles in turbulent flows. However this does not seem the case. Indeed a detailed theoretical analysis for the motion of inertial particles in these vortical structures had already been done by Marcu et al.; the present paper reproduces one of possible scenarios of the model with suitable parameters, without adding new knowledge.

Moreover, since the work of Marcu et al., there has been a considerable amount of research about statistical characterisation of inertial particle spatial distribution in turbulent flows. Many different analysis in terms of deviations from Poisson distribution,

Radial Distribution Function or Voronoi diagrams, have been applied to the case of polydisperse solutions also (see e.g. 2012 New J. Phys. vol. 14, 095013). Let me stress that voids appear at scales which are about 20-40 Kolmogorov scales, so distances at the edge between the dissipative and the inertial ranges of turbulence, where the strongest intermittent fluctuations take place. To summarise: turbulence at small scales is very different from a superposition of Burgers vortices, the use of simplified models can be accepted at a qualitative level to make things clearer but can not replace statistical analysis. Since the observations are interesting and worth of publication, I suggest the authors to perform additional work and to make a considerable revision of the manuscript.

**We agree with te reviewer that we use a simplified Burgers vortex model exploited by Marcu to explain the experimental data. However, the original work of Marcu is just one of many theoretical models. First of all we used it to explain behavior of polydysperse particles inside a vortex and this had not been done before. What is even more important, we validate theoretical approach by an observation of a particular phenomenon - cloud voids.**
**We agree that turbulence at small scales is very different from a superposition of Burgers vortices. The use of simplified models can be accepted at a qualitative level to make things clearer but can not replace statistical analysis of droplet spatial distribution in 3D turbulent flow. Nonetheless there are just a few analysis specific of cloud droplets in small scales, no 2D or 3D data on cloud droplets spatial distributions in the domains of void size and larger, not to mention simultaneous measurement of droplet position and size. Our analysis shows, that existence of Burgers-like vortices in the measurement conditions are likely and they may explain observed phenomenon, which adds certainly new knowlegde. We make an effort to improve the manuscript and present our intensions in more clear way.**

Detailed comments

1. Starting from the Abstract and then few times in the paper, authors speak about sorting effect. What is it? Can they state clearly what is the sorting effect and how it is different/similar to the preferential concentration effect? **We define clustering of particles as inhomogeneous distribution of particles in space. Preferential concentration (or preferential sampling) is specific kind of clustering: particles sample certain regions of the flow, so there is correlation between particle spatial distribution and spatial distribution of a flow characteristic/s. The term "sorting" was in fact used interchangeably to "segregation" which describes polydisperse statistics: spatial distribution of different sized particles are anticorrelated. To make our point about clustering and sorting in vortex tube clear these explanation was incorporated in the manuscript.**

2. In Section 2, the authors should detail what are the Mie scattering visual effects. These are often called as possible co-responsible for the creation of voids, but there are not data or analysis related to them. Have these effects been observed in laboratory experiment? Can we reproduce similar conditions? Either the authors better detail what they have in mind, or it is better to simply mention the problem once.

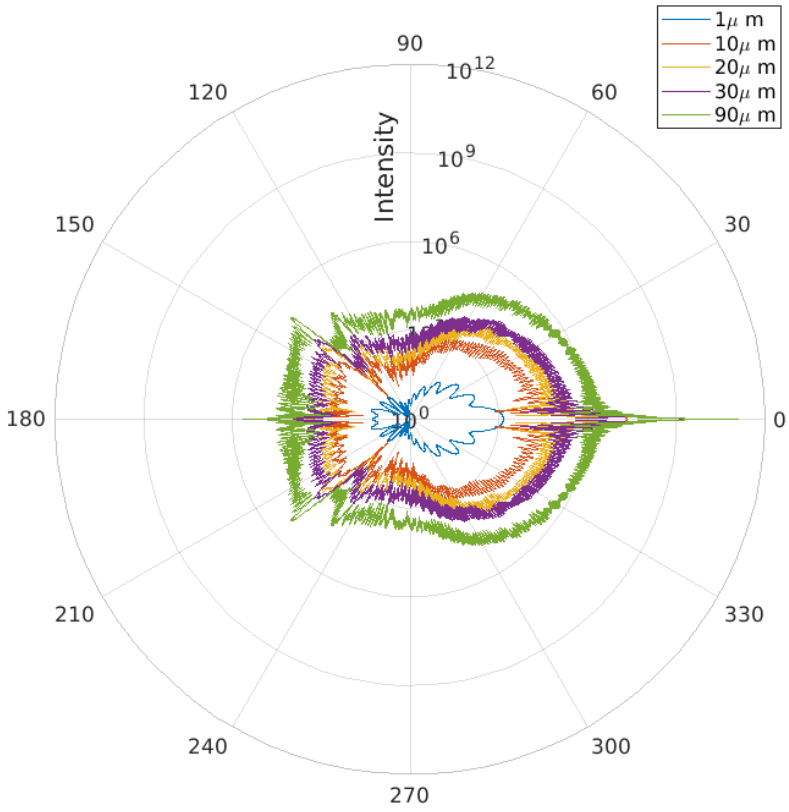


**Figure 1.** Relative scattered light intensity versus angle for a water droplet in the air. Colors correspond to different droplet radii.

**To clarify this point we added a paragraph about Mie scattering role in particle imaging and its potential influence on void observation. Mie scattering theory (van de Hulst, 1957) was validated experimentally with the accuracy far beyond our use (Harris, 1969). There is as well a great extent of literature devoted to Mie theory and its applications in experiments using scattering on particles both in the laboratory flows and in the atmosphere (see for example Dyer et al. (2006), Graßmann and Peters (2004), Fischer (2017)). The exact impact on particle tracking and sizing in imaging experiments performed in atmospheric conditions is an area of current research. We are definitely not able to reproduce in the laboratory conditions similar to those described in the paper in the laboratory. Hence we cannot measure directly the Mie scattering influence on void creation. What we know is that the intensity of scattered light is nonlinear with particle size and the angle of scattering, what we present in Fig.1 here. Nonetheless we formulate the hypothesis of its great influence on vortex finall image with the aim to sensitize to potential bias it may cause in the interpretation of observations.**

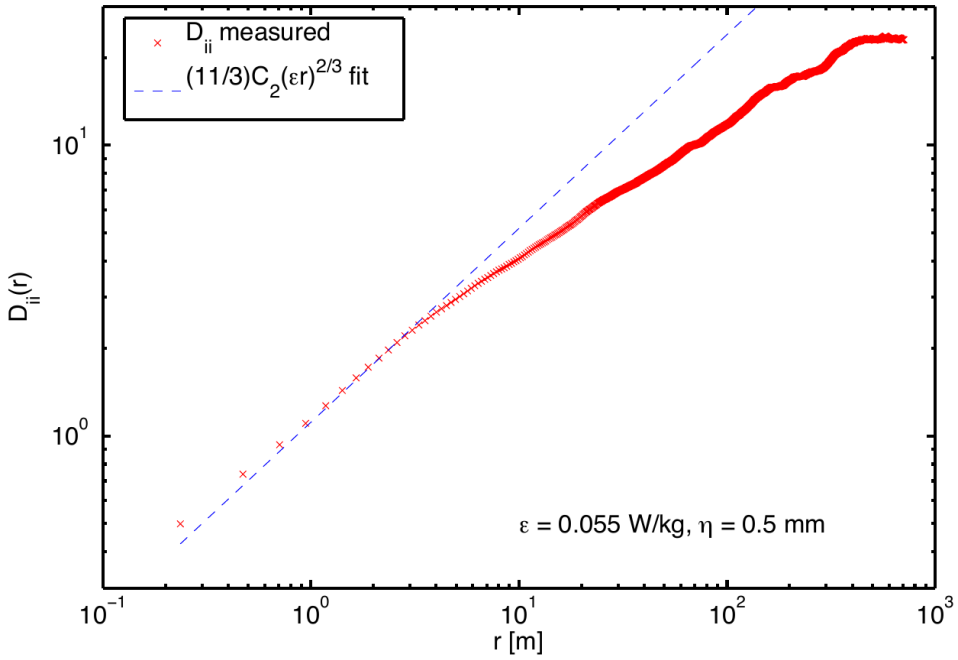


**Figure 2.** Turbulence masurement second order velocity structure functions during the cloud void event of 27th August, from MPIDS sonic sensors (sampled at 10Hz)

Also in Section 2, they mention that the "velocity structure functions were calculated using Taylor's frozen-flow hypothesis, and the energy dissipation rates were determined using inertial range scaling". Can they show these data to see the extent of the inertial range both for the temporal and the spatial scales?

**We provide the structure functions plots made for data aquired during cloud void events in Fig.2 and 3 here. Generally the experimental conditions were similar to these discussed in detail in Risius et al. (2015), and presented in Fig. 10 there. Obviously, lower part of the inertial range is not resolved there. Hot wire measurements, resolving smaller scales are discussed in Siebert et al. (2015).**

3. At the end of page 4, the authors mention that they selected 27 voids for further analysis. Are these statistically equivalent? Can the authors perform a statistical analysis of the way droplets distribute in space? See comments above.

**The reason for publishing the observations of voids described in this paper is that they were unique. They were conducted in the brain-storming process and the consequence of this fact is that they lack certain dilligence. The data collected does not certainly allow for analysis of droplets distribution in space. Due to the specific difficulty connected to the measurements conducted in the atmosphere there is no reliable literature data about 2D cloud droplets distributions ranging to inertial scales whatsoever. The data collected suggest that turbulence conditions and droplet size distributions were quite steady in the course of the void observations and we are convinced this**

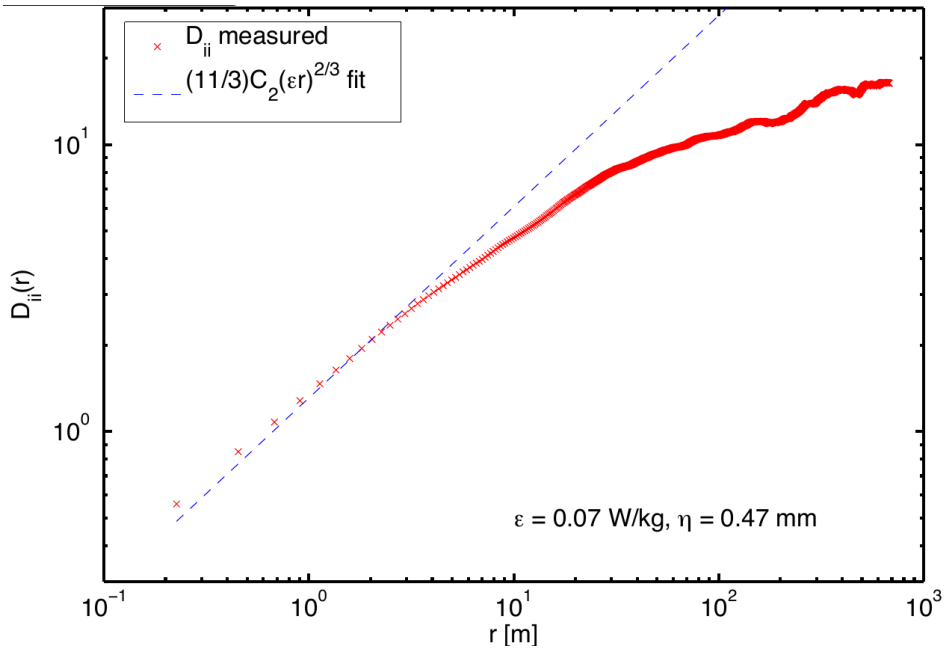


**Figure 3.** Turbulence masurement second order velocity structure functions during the cloud void event of 29th August, from MPIDS sonic sensors (sampled at 10Hz)

**allowes us to compare these voids as they were statistically equivalent. Even if it is not the case the sheer information of their existence, approximate size and a proof they may not be the result of edge effect is a complete novelty and should be published to inspire future more thorough investigations.**

4. Table I should be enriched with turbulent flow parameters such as the value of the Taylor scale Reynolds number $Re_\lambda$, the value of the Kolmogorov scale $\tau$, estimate for large-scale eddy-turn-over-time $T_L$ and correlation length $L$, the expression used for St and Sv. **The Kolmogorov scale $\tau_\eta = \sqrt{\nu\epsilon^{-1}}$ was added to the Table 1. Stokes number and sedimentation parameters were estimated using the expressions $St = \tau_p\tau_\eta^{-1}$, $Sv = \tau_\eta\tau_g^{-1}$, where $\tau_p$ is particle inertial response time, $\tau_g = \eta(g\tau_p)^{-1}$ is a time of sedimentation through the vortex. The adequate explanations are added in the text. We do not have reliable estimates of the other parameters.**

5. Pages 8 and beyond: I would suggest that values such as $A_{cr} = 0.02176$ or $r_i = 2.1866$ to be put in a table, they have no special physical meaning (only within the Burgers vortex model).
**Values were put in the table as suggested.**

6. Section 4 is not clear and moreover as the authors specify: "Different scenarios of particle motion determined by above stability conditions were shown in Fig.4 in Marcu et al. (1995). Fig. 4 here presents a simplified illustration of one of the scenarios: three equilibrium points, unstable point near the axis, stable point far from the axis, and droplets

rotating around the vortex center." How are the other scenarios excluded? What is special in the one chosen? **Fig.4 was included in the paper for illustrative purposes. We show particle trajectories around equillibrium points of different stability properties in the simplest way without copying the original image. Presenting the chosen scenario fulfills this goal and helps in the discussion.**

7. Here the whole analysis can also be made much shorter, and summarised in terms of the very natural rough conclusions mentioned at the end of page 11. Details can be moved in an appendix.
   **The other reviewers asked for more details in the analysis and that is the reason we decided to leave it in the main text body.**

8. Authors want to reproduce observations of August 27: from figure 1 it is the day with a very broad radii distribution. Have they used this shape to initialise the numerical simulations? Or can they superpose the shape they used to the experimental one? This is not clear from the text and the sentence "A semi-Gaussian distribution of droplet radii cut off at R = 1.5um was chosen for simulations to match the experimental values from the 27th of August (see Table 1)" without further details does not clarify the point.
   **We used the gaussian distribution as presented in Fig 4 here. Havng received this remarks we decided to change in the simulations the gaussian distribution to the one measured.**

9. The work reports about void/clustering effects of inertial particles in turbulent flows but many relevant papers for the topic are not cited. To mention just a few: Collins and Keswani, 2004 New Journal of Physics 6 (1), 119; Bec et al. 2007 Phys. Rev. Lett. 98, 084502; Monchaux, Bourgoin, and Cartellier, 2010 Phys. Fluids 22, 103304.
   **The thorough review of the research on clustering was not our intention. We mentioned only the papers that described different important clustering mechanism. We rephrased it in the conclusions and we hope it is now clear.**

10. A number of typos are present.

**Review 3**

This is an interesting article with some novel field data and numerical results which have been interpreted with reference to existing theoretical analysis. The extent to which this analysis is strictly applicable to real clouds is perhaps moot but it nevertheless provides a useful starting point and appropriate orders of magnitude. I would recommend publication but found aspects of the paper, particularly the summary of the analysis (§3) and its application (§4) confusing.

I have a number of detailed points, mostly minor, which I would like the authors to consider especially with a view to improving the clarity of their arguments. I have also made a number of suggestions for improving the written English.

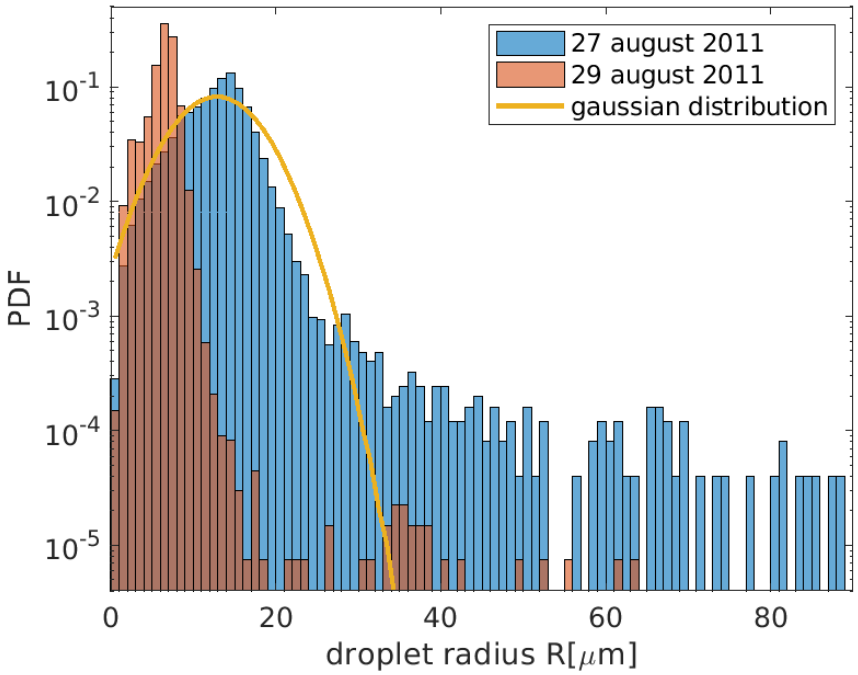


**Figure 4.** Droplet size distributions measured with PDI probe (blue and red) with gaussian distribution cut at $R = 0$ superimposed.

Detailed comments

1. p.3, l. 29 It's not clear what 'They' in the sentence 'They were smaller ...' is referring to here: 'Swiss cheese' or 'cloud holes' ?

**It was referring to cloud holes. This part was rephrased.**

2. p.6, eq. (2) Could the authors provide a reference for this? Or at least some more motivation?

**The reference to the original work of Burgers was provided.**

3. p.9, l. 2 What is $r_0$? Does it have any physical relevance? It would be helpful if $\varphi(x)$ were defined so that its dependence on the parameters in the problem is made clear; it has an important role in the analysis.

**$r_0^*$ is just the notation for arbitrary solution of the Eq.6. The function $\varphi(r_0^*)$ has no parameters. It was added expicitely in the text.**

4. p.9, l.12 I didn't understand the sentence beginning 'Particle motion ...' especially 'separated from the motion 2D space'.

**It means that equations describing particle motion in the plane perpendicular to the vortex axis separate from the equation describing motion along vortex axis. This part was rewritten to make it clear.**

5. p.11, eq. (9) For the linearization of eq. (6) I obtained (). While this differs from eq. (9) for non-zero $A$, it does give me $r^* = 4\pi Sv$ in the limit $A \to 0$ in agreement with eq. (9).

**We provide this calculation in the revised manuscript.**

6. p.11, l.16 I didn't understand the first sentence '... splits in parts'. Two parts?

**This part was rephrased accordingly.**

7. p. 11, l. 23+ Why are the conclusions 'rough' ? I didn't follow all of the logic here: as the influence of gravity increases i.e. $gsin\theta$ increases or the vortex core size, $\delta$, increases (or both) then $B$ decreases. Decreasing B means decreasing Amax which is consistent with increasing $\Gamma$ (circulation). My understanding is that $A < A_{max}$ for void creation. So as either $gsin\theta$ or $\delta$, (or both) increase it becomes harder for voids to form unless the circulation increases appropriately. So I agree with the first conclusion so long as increasing minimum circulation equates to decreasing $A_{max}$ .
**We reformulated the text to make the understanding easier. Increasing minimum circulation equates to decreasing $A_{max}$ so conclusions are the same as before.**

A further consequence of decreasing $B$ is decreasing $St_1$ and $\Delta St$ since the latter is proportional to $B^{1/3}$. This implies that, for fixed $\tau_f$ (circulation), the minimum particle size decreases with decreasing $B$ as the second point suggests though it is not written very clearly. Since $\Delta St$ decreases with decreasing $B$ this suggests the range of particle size decreases with decreasing $B$ as suggested by the latter part of the third point. But decreasing $B$ corresponds to increasing $\Gamma$ which seems to contradict the first part of the third conclusion. Perhaps I have missed something in the analysis of par. 3 and 4; I would welcome more explanation.
**$\tau_f$ is not circulation (it depends on the vortex core size $\delta$ as well). We think this misunderstanding caused the confusion. Total circulation of Burgers vortex is $\Gamma = \nu/A$.**

8. p.12, l.5 The last part of this sentence doesn't read well.
**It was rewritten.**

9. p.12, §6 Which equations are the numerical simulations solving? A Burgers vortex or the Navier-Stokes equations?
**The simulations were solving particle motion equations in Burgers vortex field. It was stated explicitely in the text in section 5.**

10. p. 12, l. 32 Z and D should be defined: are they imposed on the simulation or simply typical values?
**The values were imposed on the simulations to let us account for the void creation of sizes similar to observed.**

11. p.16, l.14 My understanding of the analysis of par.3 and 4 is that $A < A_{max}$ for void creation yet here you are saying the opposite.
**The simulation set 2) in previous version was made with a mistake. The manuscript was changed in such a way that it does not present simulations with $A > A_{max}$ any more.**

**Review 4**

The paper presents field experimental observation of the so defined "cloud voids" and attempts to provide physical mechanism for this phenomena based on the simple model of inertial particle expulsion from strong, thin coherent vortices, using Burger vortex as model. The field observation of the cloud voids is in itself new and interesting and worth disclosing. However, the link to expulsion from coherent vortices is, although plausible, not as convincing as suggested in the Abstracts and Conclusion of the paper. I would recommend a somewhat weaker conclusion unless more work is done to strengthen this interpretation.
**We weakened the conclusion in the accordance to the reviewer suggestion**

In relation to this and other weaknesses, below are my detailed comments:

1. According previous works such as the cited Mouri et al (2000), coherent intense vortices are observed to have diameter not more than about 20 times the Kolmogorov microscale (as reported by Mouri et al.). This is consistent with the authors' own survey as they wrote "proportionality constant in Eq. 1 is in the range $m \in [3.5, 24]$". Their observed void size (centimeters) in this report is however about a hundred times the corresponding Kolmogorov length (see Table 1.). This calls for an explanation. E.g. are larger vortices expected in atmospheric conditions?
**We distinguish between the visible void size, dependent on effect of Mie scattering and vortex radii (Tab.3) which is close to 1cm, e.g 20 times of the Kolmogorov size in accordance to Mouri et al.**

2. As the authors stated, these coherent vortices are "severely intermittent". What could be said on the prevalence of the observed voids at the site? And could this be reconciled with known intermittency, perhaps in terms of "large-scale organization of the small-scale intermittent structures" ?
**We do not have enough documented observations to discuss this issue.**

3. Ideally, it would be very helpful, if the velocity or vorticity field around the observed void is also concurrently estimated if not measured. If that is not the case, it would be helpful to establish the presence of intense vortices, long lived enough

and having similar diameters under similar conditions, at the site.

**Unfortunately, turbulence as ocurred in the experimental site cannot be reproduced in the laboratory. The authors are working on the better instruments (light-sheets and visualization techniques), reliably working in harsh experimental environment to collect more data.**

4. The Stokes number used in simulation 1) is $St = 1.45$. I was hoping to see St similar to the experimental value (similarly for $S_v$) for a better comparison (is this not the purpose, why?, in any case I recommend that). In relation to this, I don't know if it is meaningful to claim "visible void radii are rather $\approx 2 - 2.5\ cm$, which seems close to the experimental values" (line-4, pg.16) when parameters are not matched.

   **Our purpose was to prove that simulating an image of a void of diameter close to experimentally observed is possible. Calculation of $St$ and $Sv$ both use vortex characteristic times: turnover time and sedimentation time. In 3D real turbulence flow estimates of $St$ and $Sv$ are based on Kolmogorov timescale which is a global value. The single vortex in intermittent flow however can have completely different local parameter values. Comparison of this numbers was provided rather to convince the reader that they cannot use them as leading indicators of particle behaviour. We elaborate on this topic in the text. Please note that the numerical simulation examples changed in the revised manuscript (simulation set 1) is almost the same, but simulation set 2) differs from the one before).**

5. I have difficulties understanding Figure 5 and the corresponding explanation in the text. In particular, I am not sure how to interpret the dashed-lines. Better exposition is welcomed here.

   **Dashed lines present contours of periodic orbit radius solutions for a few chosen orbit radii: 0.5 cm, 1.5 cm, 3cm. Colors refer to particle size for which this contours were calculated. We reformulated the whole paragraph and we hope it is now clear.**

6. Line-15, pg 16: "Comparison of the modeled and observed voids led . . ..". observe refers to the field data or the "visible void" in the simulation?

   **It refers to the field data. It was clarified in the text.**

7. Line-4, pg.16 : "0-1.5 cm; however, . . .." . Is zero a typo here?

   **Yes, this was a typo.**

## References


Dyer, S. D., Dennis, T., Williams, P. A., Street, L. K., Etzel, S. M., Espejo, R. J., and Milner, T. E.: High sensitivity measurements of the scattering dispersion of phantoms using spectral domain optical coherence tomography, https://doi.org/10.1117/12.649180, https://doi.org/10.1117/12.649180, 2006.

Fischer, A.: Imaging Flow Velocimetry with Laser Mie Scattering, 2017.

Graßmann, A. and Peters, F.: Size Measurement of Very Small Spherical Particles by Mie Scattering Imaging (MSI), Part. Part. Syst. Charact., 21, 379–389, https://doi.org/10.1002/ppsc.200400894, https://onlinelibrary.wiley.com/doi/abs/10.1002/ppsc.200400894, 2004.

Harris, F. S. J.: Particle characteristics from light scattering measurements, Tellus, 21, 224–229, https://doi.org/10.3402/tellusa.v21i2.10076, https://doi.org/10.3402/tellusa.v21i2.10076, 1969.

Risius, S., Xu, H., Di Lorenzo, F., Xi, H., Siebert, H., Shaw, R. A., and Bodenschatz, E.: Schneefernerhaus as a mountain research station for clouds and turbulence, Atmospheric Measurement Techniques, 8, 3209–3218, https://doi.org/10.5194/amt-8-3209-2015, http://www.atmos-meas-tech.net/8/3209/2015, 2015.

Siebert, H., Shaw, R. A., Ditas, J., Schmeissner, T., Malinowski, S. P., Bodenschatz, E., and Xu, H.: High-resolution measurement of cloud microphysics and turbulence at a mountaintop station, Atmospheric Measurement Techniques, 8, 3219–3228, https://doi.org/10.5194/amt-8-3219-2015, http://www.atmos-meas-tech.net/8/3219/2015, 2015.

van de Hulst, H. C.: Light scattering by small particles, p. 470; 103, https://doi.org/10.1002/qj.49708436025, https://rmets.onlinelibrary.wiley.com/doi/abs/10.1002/qj.49708436025, 1957.

# Turbulence Induced Cloud Voids: Observation and Interpretation

Katarzyna Karpinska[1], Jonathan F.E. Bodenschatz[2], Szymon P. Malinowski[1], Jakub L. Nowak[1], Steffen Risius[2], Tina Schmeissner[4], Raymond A. Shaw[3], Holger Siebert[4], Hengdong Xi[2], Haitao Xu[2], and Eberhard Bodenschatz[2]

[1]Institute of Geophysics, Faculty of Physics, University of Warsaw, Warsaw, Poland
[2]Max Planck Institute for Dynamics and Self-Organization, Goetingen, Germany
[3]Michigan Technological University, Houghton, Michigan, USA
[4]Leibniz Institute for Tropospheric Research, Leipzig, Germany

**Correspondence:** S. P. Malinowski (malina@fuw.edu.pl)

**Abstract.** The phenomenon of "cloud voids", i.e., elongated volumes inside a cloud that are devoid of droplets, was observed with laser sheet photography in clouds at a mountain-top station. Two experimental cases, similar in turbulence conditions yet with diverse droplet size distributions and cloud void prevalence, are reported. A theoretical explanation is proposed based on the study of heavy inertial sedimenting particles inside a Burgers vortex. A general conclusion regarding void appearance is drawn from theoretical analysis. Numerical simulations of polydisperse droplet motion with realistic vortex parameters and Mie scattering visual effects accounted for can explain the presence of voids with sizes similar to that of the observed ones. ~~Preferential concentration and sorting~~ Clustering and segregation effects in a vortex tube are discussed for reasonable cloud conditions.



## 1 Introduction

The dynamics of heavy inertial particles in turbulent flow is a universal problem that appears in astrophysics, oceanography, engineering and atmospheric sciences. In particular, in cloud physics, deeper understanding of the interaction between atmospheric turbulence and cloud droplets is seen as a potential answer to many important questions (Bodenschatz et al. (2010)). Over the years, there has been considerable speculation about the possible role of coherent, long-lived vortex structures in cloud turbulence and microphysical processes, including both ~~condensation~~ condensational growth and collision-coalescence growth (see Tennekes and Woods (1973), Maxey and Corrsin (1986), Shaw et al. (1998), Shaw (2000), Markowicz et al. (2000), Hill (2005)). This paper describes the first ~~experimental~~ in situ observation of a phenomenon we refer to as “cloud voids" - cylindrical volumes devoid of droplets recorded in real clouds - and is focused on determining whether inertially induced voids indeed may occur in clouds due to the presence of strong vortex structures.

Vortex tubes, sometimes called “worms", are severely intermittent, coherent, elongated and long-lasting structures characteristic of high Reynolds number turbulent flows (e.g. Mouri et al. (2000)). Past theoretical and experimental studies lack general conclusions about their characteristic time and length scales, intensity and appearance in turbulence. In particular, most of the research was conducted under conditions different from multiscale atmospheric turbulence. Statistical analysis based on such research (see e.g. Jiménez et al. (1993), Belin et al. (1999), Pirozzoli (2012)) showed that Burgers vortex core size $\delta$ (defined later in Eq. 2), scales roughly with the Kolmogorov length scale $\eta$:

$$\delta = m\eta \tag{1}$$

and that $m$ has a distribution ranging from a few to a few tens with its mean around $m = 4$. Moisy and Jimenez (2004) analyzing DNS instant velocity fields propose that vorticity structures' geometrical aspect ratios evolve towards long tubes (1:1:10) with increasing vorticity threshold. What is more they show that these structures concentrate into clusters of the size in inertial range of scales. This implies the presence of large-scale organization of the small-scale intermittent structures. In the study by Biferale et al. (2000), statistics of vortex filament lifetime for a low Taylor microscale Reynolds number $Re_\lambda$ indicate that the maximum lifetime is on the order of the integral timescale, whereas its mean scales with the Kolmogorov timescale. Numerical experiments described in Tanahashi et al. (2008) suggest that there is a relation between root mean square velocity fluctuations and the circulation parameter $\Gamma$ of a vortex tube modeled as a Burgers vortex.

Previous efforts to study dynamics of heavy, inertial particles in vortices were made by simulating droplet trajectories in a prescribed velocity field for several simple single vortex models. Such research for the simplest model of a line vortex with stretching was conducted by Markowicz et al. (2000) with limitation to horizontally oriented vortices. In order to better understand the problem of cloud droplet dynamics in atmospheric conditions the same model but with arbitrary gravity alignment was studied by Karpinska and Malinowski (2014). Another model, free from the problem of unrealistic singularity on the vortex axis, is a Burgers vortex with stretching. It is commonly seen as a very good approximation of a real vortex tube (Neu (1984), Jimenez and Wray (1998)). The specific features of droplet motion for monodisperse droplets in a Burgers vortex were examined by Hill (2005) for horizontal alignment and by Marcu et al. (1995) for arbitrary alignment with respect to gravity.

Clustering and segregation effects are of importance when talking about interaction between particles and turbulent flow. We define clustering of particles of arbitrary sizes as inhomogeneous distribution of particles in space. Segregation refers to the cases in which spatial distribution of different sized particles are anticorrelated. Different kinds of particle clustering in turbulent flow were reviewed by Gustavsson and Mehlig (2016), turbulence-induced segregation was for example treated by Calzavarini et al. (2008).

In this paper we describe the serendipitous observation of numerous, isolated voids in clouds, while conducting measurements at a mountain-top station. The voids were visually striking and generated great excitement from the scientific team. Here, we present direct, 2D observations of the distinct types of patterns of clear air in clouds, along with accompanying turbulence and cloud microphysical measurements. We pose the question of whether the observed cloud voids are consistent with inertial

droplet response to turbulence under atmospheric conditions. To answer this question, analysis of the particle dynamics in a Burgers vortex is further developed for the heavy sedimenting polydisperse case and the model is interpreted in the context of the observations.

The paper is structured as follows. Section 2 describes the measurement method and analysis of experimental data that shows the phenomenon of cloud voids. Section 3 presents relevant features of single droplet trajectories in a vortex tube model. Section ~~?? continues the analysis of~~ 4 projects the analysis on polydisperse droplet motion in a vortex to define the conditions of cloud void emergence. Section ~~4.1 describes a method of finding simulation parameters corresponding to observed cloud voids, and Sect.~~ 5 outlines the influence of Mie scattering theory specifics on droplet imaging and in consequence void observation. Section 6 presents void numerical simulation results. Section 7 incorporates the discussion and conclusions.

## 2 Experimental Evidence

Intriguing structures inside clouds, as presented in Fig. 1, were recorded by means of laser sheet photography during observations performed on 27 and 29 August 2011 at Umweltforschungsstation Schneefernerhaus (UFS) on the slopes of Mt. Zugspitze in the German Alps. Each time, the cloud event lasted for several hours. For a description of the observatory and characterization of the cloud and turbulence conditions on-site, see Risius et al. (2015) and Siebert et al. (2015). Authors of these papers showed that turbulence and cloud microphysical properties at the measurement site are quite reasonable representations of measurements made in 'free' clouds away from the surface.

Clouds were illuminated by a laser sheet created with a frequency-doubled high-power Nd:YAG laser (532 nm, 45 W). The sheet was set either vertical or oblique with respect to gravity. The angle between the laser sheet plane and camera recording plane in the oblique case was chosen to increase the scattering intensity on droplets and falls within the range of 30-40 degrees. The laser sheet in the observation region was around 50 cm wide and 1 cm thick. Images covering the approximately 2 m long section of the sheet at a distance approximately 10 m from the source were taken with a Nikon D3S DSLR 12 Mpix camera.

Laser sheet photography was accompanied by high-resolution measurements of small-scale turbulence and cloud microphysics, as described in Siebert et al. (2015). Flow turbulence was measured by 3D ultrasonic anemometers operated at 10 Hz, from which the velocity structure functions were calculated using Taylor's frozen-flow hypothesis, and the mean energy dissipation rates were determined using inertial range scaling. Droplet size was measured by a PDI probe (Chuang et al., 2008) mounted approximately 6 m down from the camera level. Figure 2 presents the measurement set-up and recorded size spectra of droplets. Droplet and turbulence measurements are summarized in the Table 1. The mean values refer to 30-minute long record corresponding to the camera acquisition series.

Two kinds of events in which droplet spatial distribution is visibly inhomogeneous were distinguished in the collected images. The first kind was characterized by an irregular interface separating clear-air and cloudy-air volumes and/or cloudy

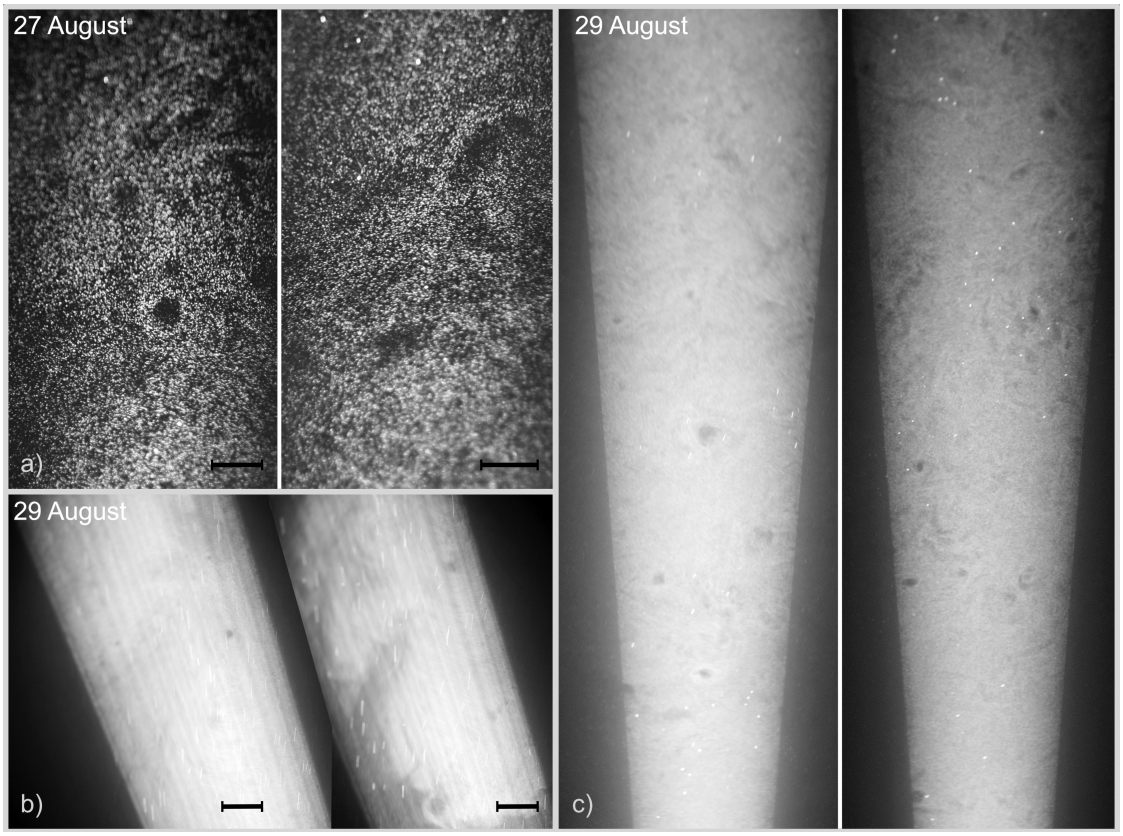


**Figure 1.** Examples of cloud voids observed at the UFS station with various camera-laser configurations. ~~Pictures~~ Images taken on 27 August (panel a) were chosen to estimate cloud void sizes. The ones recorded on 29 August evening (panel b) show the difference between inhomogeneities produced by cloud voids and those resulting from the mixing with clear air at the cloud edge. Other ~~pictures~~ images from 29 August (panel c) suggest that the voids can be quite frequent in the sample volume. Bright spots and lines are due to presence of larger precipitation particles. 10 cm long segment is shown to represent spatial scale assumed in the void size calculation. For more details, see the movies attached in the supplementary materials.

volumes of visibly different properties over a wide range of spatial scales (panel b) in Fig. 1). Inhomogeneities of the second ~~type~~kind, present within the cloudy volumes, were called cloud voids in “Swiss cheese" clouds. ~~The word "cloud holes" is avoided because it is commonly used referring to the cloud-free regions occurring in stratocumulus decks, as described for example in (?). They were smaller~~ Cloud voids were small (a few centimeters scale), the interface was usually blurry (see panels a) and c) in Fig. 1) and the shapes of clear-air regions were often close to round or elliptic (see magnified voids in Fig. 3). It is important to point that more intuitive expression "cloud holes" with regards to these inhomogeneities is avoided on purpose because it is commonly used referring to the cloud-free regions occurring in stratocumulus decks, as described for example in Gerber et al. (2005). Inhomogeneities of the first kind are argued to be created in the process of cloud – clear-air mixing ~~(Warhaft, 2000)~~(e.g. Warhaft (2000)). In contrast, in some series of images and movies, the shape of the recorded tracks of

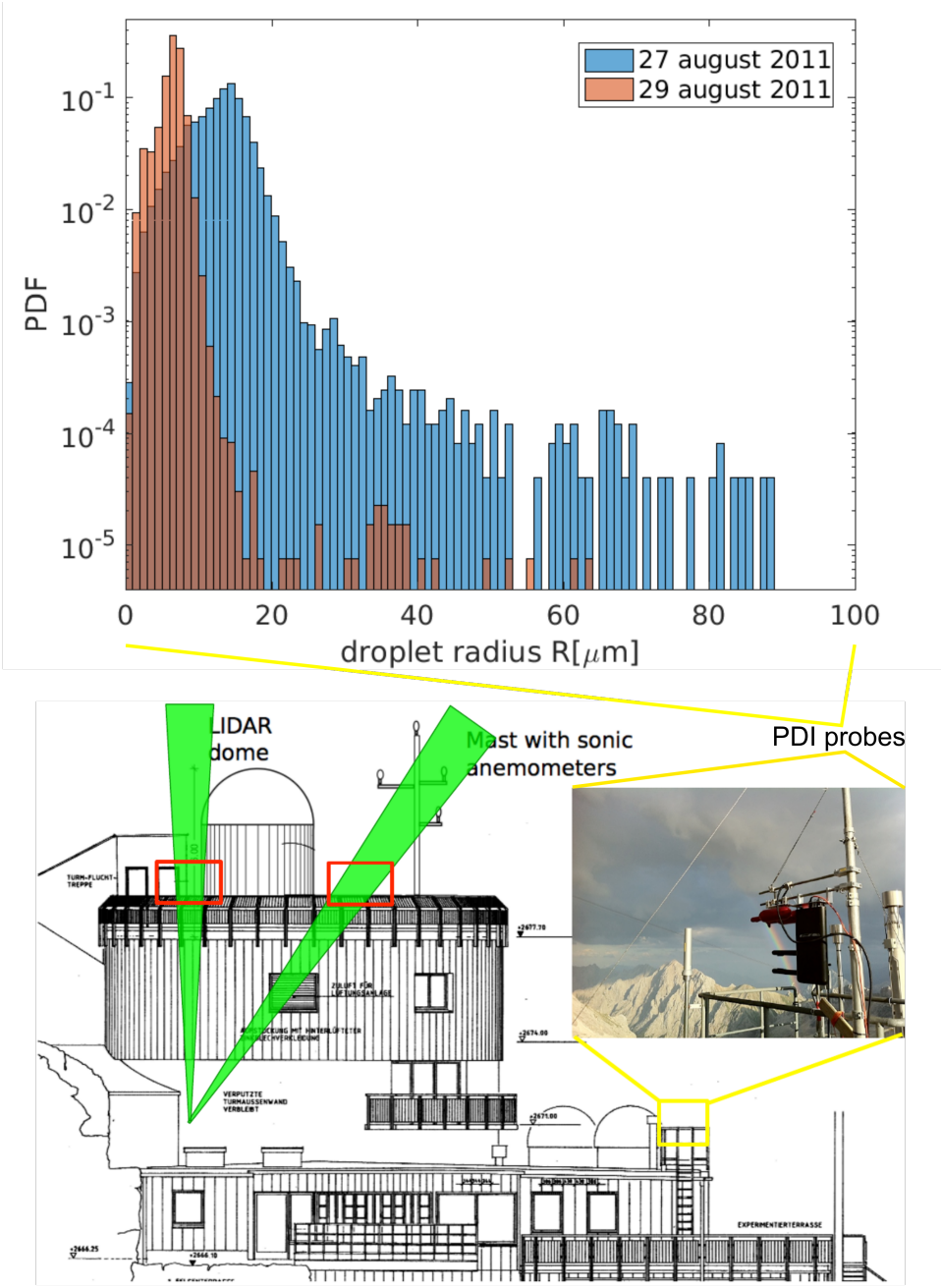


**Figure 2.** Droplet size ~~distribution~~ distributions measured with a PDI probe (top) and the arrangement of instruments at the measurement site (bottom).

cloud droplets suggest the following cloud void origin hypothesis: they result from interactions between inertial, heavy cloud droplets and small-scale vortices present in a turbulent cloud. Comparison of the two described cases becomes straightforward

**Table 1.** Properties of turbulence and cloud droplets during observation periods.

| | August 27th | August 29th |
|---|---|---|
| Energy dissipation rate $\epsilon$ [m$^2$/s$^3$] | 0.055 | 0.070 |
| Kolmogorov length scale $\eta$ [mm] | 0.50 | 0.47 |
| Komogorov timescale $\tau_\eta$ [s] | 0.017 | 0.015 |
| Mean droplet radius $R$ [$\mu$m] | 12.9 $\pm$ 4.8 | 6.4 $\pm$ 1.5 |
| Sauter mean radius $R_{32}$ [$\mu$m] | 18.1 | 7.3 |
| Stokes number $St$ (mean) | 0.126 | 0.035 |
| Stokes number $St_{32}$ (Sauter) | 0.247 | 0.045 |
| Sedimentation parameter $Sv$ | 0.676 | 0.172 |
| Froude number $Fr$ | 0.431 | 0.470 |
| Number density $n$ [cm$^{-3}$] | 56 $\pm$ 47 | no data |

when conducted on the basis of the movies in the database (Karpinska et al., 2018). In the movie "ms01" between ~~13s and 22s~~ 13 s and 22 s there are two cloud void appearances. Motion of the void in the homogeneous cloud field resembles motion of a worm. Movie "ms02" presents cloudy and clear air mixing at the cloud edges.

There were a few series of cloud void images collected with various laser-camera settings on the two experimental days. The best quality series, made in the morning of the 27th, was chosen for void size analysis. For the series of 17 photos selected for analysis, there were four in which voids were not clear enough to be accounted for. In the remaining 13 photos 27 voids were identified. Each one's size was manually determined. In the case of a round void, the diameter was taken as the size; in a case of flattened or ellipsoidal void, the maximal chord was taken. The typical void diameter was estimated to be 3.5$\pm$1 cm; the maximal, 12$\pm$4 cm; the minimal, 1$\pm$0.5 cm. Images from the analyzed series from the morning of August 27th showing examples of objects identified as voids are presented in the panel a) of Fig. 1. ~~voids~~ Voids captured on the 29th of August were not analyzed due to the large uncertainty resulting from the unknown geometry of the camera-laser set-up. The general experimental observation was that the voids were smaller then those on August 27th. Definitive experimental verification of the cloud void origin is not possible on the basis of collected data only; however, in next sections, we argue that void creation due to inertia of droplets present inside vortex tubes is highly probable.

## 3 Motion of Heavy, Inertial Particles in the Vortex Tube Model

To address theoretically the issue of cloud void origin, we follow the concept of the polydisperse inertial droplet population response to a coherent vortex pattern. In this section we take the first step on this track presenting relevant features of single droplet trajectory in the chosen vortex tube model. A population of particles is assumed to form a dilute collection of material points, heavy and inertial, displaced by gravity force and viscous force (Stokes drag) only. Burgers vortex (Burgers, 1948) is

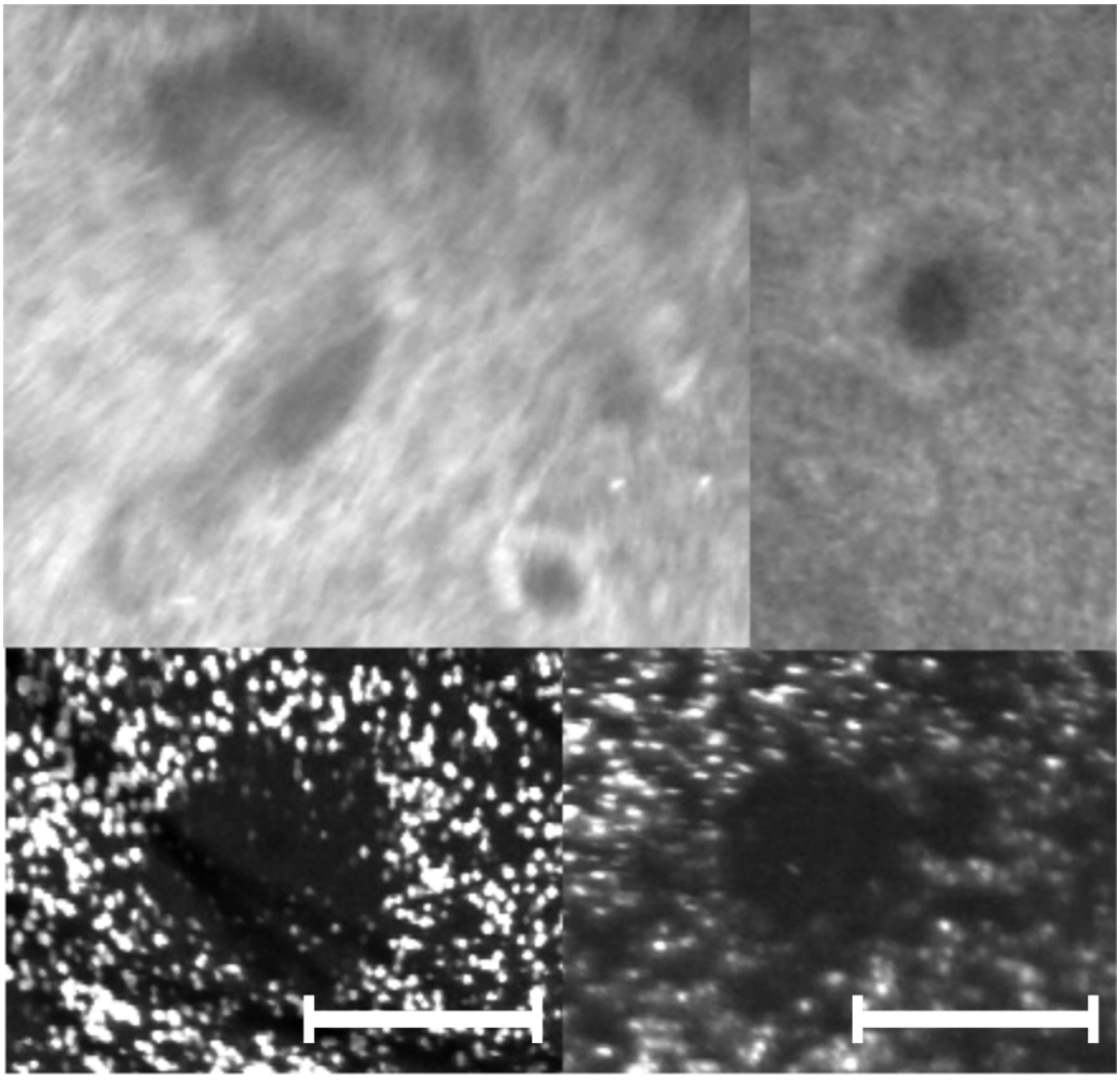

**Figure 3.** Example close-ups of variously shaped cloud voids observed at the UFS station with different camera-laser configurations. 5 cm long segment is shown to represent spatial scale assumed in the void size calculation.

used as a model of a steady vortex tube. The $z$-axis in the cylindrical coordinate system $(r, \varphi, z)$ is aligned with the vortex axis. ~~Its~~ 3D velocity field $\boldsymbol{v}$ is determined by two parameters: circulation $\Gamma$ and stretching strength $\gamma$:

$$\boldsymbol{v} = -\frac{\gamma}{2} r \hat{e}_r + \frac{\Gamma}{2\pi r}\left(1 - e^{-\frac{r^2}{2\delta^2}}\right)\hat{e}_\varphi + \gamma z \hat{e}_z, \tag{2}$$

where $\delta = \sqrt{2\nu/\gamma}$ is the vortex core size and $\nu$ denotes the kinematic viscosity. A particle's equation of motion is as follows:

$$\ddot{\boldsymbol{r}} = \frac{1}{\tau_p}(\boldsymbol{v} - \dot{\boldsymbol{r}}) + \boldsymbol{g}, \tag{3}$$

where $\tau_p$ is the particle relaxation time and $\boldsymbol{g} = -g(\sin\theta\hat{e_y} + \cos\theta\hat{e_z})$ is gravitational acceleration inclined by the angle $\theta \in [0, 90^o]$ with respect to the vortex axis.

The analysis of single droplet motion in projection on a plane $(r, \varphi)$ perpendicular to the vortex axis (henceforth called 2D space) was conducted by Marcu et al. (1995) and is summarized below. The behavior of a droplet inside the vortex depends on a set of six parameters $\{\Gamma, \gamma, \theta, \tau_p, g, \nu\}$. The nondimensionalization of the equations leads to Eq. 4 and gives a set of dimensionless parameters $\{St, Sv, \theta, A\}$:

$$\begin{cases} \ddot{r^*} - r^*\dot{\varphi^*}^2 = -St^{-1}\left(Ar^* + \dot{r^*} + Sv\sin\varphi\right) \\ 2\dot{r^*}\dot{\varphi^*} + r^*\ddot{\varphi^*} = St^{-1}\left(\frac{1}{2\pi r^*}(1 - e^{-\frac{r^{*2}}{2}}) - r^*\dot{\varphi^*} - Sv\cos\varphi\right) \\ \ddot{z^*} = St^{-1}\left(Az - \dot{z^*} - Sv\cot\theta\right) \end{cases}. \tag{4}$$

Henceforth, dimensionless variables are denoted by $^*$. Stokes number $St$ ~~was~~ here is calculated with the use of the characteristic timescale of the Burgers vortex flow, which is the vortex core rotation time $\tau_f = \delta^2\Gamma^{-1}$, so $St = \tau_p\tau_f^{-1} = \tau_p\Gamma\delta^{-2}$. The sedimentation parameter $Sv$ is a ratio of $\tau_f$ to the timescale of sedimentation through the vortex: $Sv = \tau_f\tau_g^{-1} = \delta g\tau_p\sin\theta\Gamma^{-1}$. It characterizes motion in a plane perpendicular to the vortex axis. The last quantity ~~$A = \nu\Gamma^{-1}$ is the strain parameter~~ $A = \nu\Gamma^{-1} = 1/Re_v$ is the nondimensional strain parameter, the inverse of vortex Reynolds number $Re_v$. It is worth mentioning that the ratio of Stokes number to the sedimentation parameter, called Froude number $Fr = StSv^{-1}$, is a measure of the influence of gravitational force on the droplet motion. In the limit of a large Froude number, gravity is considered negligible.

As one can see in Eq.4 equation describing particle motion along the vortex axis is separated from the equations describing motion in 2D space.

### 3.1 Motion along the vortex axis

Motion along the vortex axis is determined by stretching outflow drag and gravity force. As a consequence particle $z$ position shows an exponential dependence on time. What is more, every droplet has one unstable equilibrium point at $z_0^* = SvA^{-1}\cot\theta = \nu^{-1}g\delta\tau_p$. The analytical solution was presented in (Karpinska and Malinowski, 2014).

### 3.2 Motion in the plane perpendicular to vortex axis

The solutions of ~~the above equations~~ Eq.4 have several different attractors in 2D space~~(valid for 3D case without gravity or with gravity~~. It is helpful to distinguish two cases: with gravity and without gravity (valid as well when gravity is parallel to the vortex axis).

=0.2cm

**Table 2.** Existence of equillibrium points with respect to $A$ and $Sv$ parameters. $A_cr$, $r^*_s$, $r^*_{min}$, $Sv_{min}$, $Sv_{max}$ defined in the text body.

| | | |
|---|---|---|
| $A \geq A_{cr}$ | Sv - arbitrary | 1 eq. point |
| $A < A_{cr}$ | $< Sv_{min}$ | 1 eq. point at $r^* < r_s$ |
| | $[Sv_{min}, Sv_{max}]$ | 2 or 3 eq. points |
| | $> Sv_{max}$ | 1 eq. point at $r^* > r_{min}$ |

### 3.2.1 Without gravity (vertical vortex)

For every particle of a given radius a stable, circular periodic orbit exists if $St < St_{cr} = 16\pi^2 A$. For $St \geq St_{cr}$, there exists a stable equilibrium point positioned on the vortex axis. A radius of the periodic orbit satisfies the equation:

$$r^{*2}\sqrt{A/St} - \left[1 - \exp\left(-r^{*2}/2\right)\right]/2\pi = 0. \tag{5}$$

### 3.2.2 With gravity (inclined vortex)

Nonparallel alignment of the gravity vector and vortex axis ($\theta \neq 0$) destroys the axial symmetry of the system and introduces the presence of other attractors, such as limit cycles and equilibrium points outside the axis.

For a nonzero $\theta$, every particle always has equilibrium points in 2D space. Positions of these points are determined by $Sv$ and $A$. They can be obtained by solving the equation for the radial component $r^*$:

$$r^* A \sqrt{1 + \left(\frac{1 - \exp\left(\frac{-r^{*2}}{2}\right)}{2\pi A r^{*2}}\right)^2} = Sv. \tag{6}$$

Now, let $f_A(r^*)$ be the left hand side of Eq. 6. A plot of this function for a given $A$ is called ~~a~~ an equilibrium curve (see Fig.2 in Marcu et al. (1995)). Detailed analysis of equillibrium curve dependence on parameters is performed below and leads to the conclusions summarised in the Table 2.

It is easy to find that $f_A(0) = 0$ and $\lim_{r^* \to \infty} f_A(r^*) = \infty$. Moreover, there exists a critical value ~~$A_{cr} = 0.02176$~~ $A_{cr}$ for which bifurcation from one unique solution (for $A \geq A_{cr}$) to maximally three solutions (for $A < A_{cr}$) occurs. $A_{cr}$ corresponds to equillibrium curve that has a horizontal slope at the inflection point. $A_{cr}$ value was estimated numerically (see the Table 3). For $A \geq A_{cr}$ the equilibrium curve is a monotonically increasing function ~~so there is exactly one $r^{ast}$~~ of $r^*$ so there exist exactly one solution for every $Sv$ value. For $A < A_{cr}$ the equilibrium curve always has one maximum at $r^*_{max}$ and one minimum at $r^*_{min}$. The inflection point at $A = A_{cr}$ on the equilibrium curve ~~, which lies at $r^*_i = 2.1866$,~~ lies at $r^*_i$ (see the Table 3). It restricts values of $r^*_{max}$ from above ~~,~~ and values of $r^*_{min}$ from below. Consequently, for $Sv < f_A(r^*_{min})$ and for $Sv > f_A(r^*_{max})$, there

=0.2cm

**Table 3.** Burgers vortex nondimensional numbers

| | |
|---|---|
| $A_{cr}$ | 0.02176 |
| $r_i^*$ | 2.1866 |
| $r_s^*$ | 1.585201 |
| $A_t$ | 0.01917 |

is only one solution. For ~~$Sv = f_A(r^*_{min})$ and for $Sv = f_A(r^*_{max})$~~ $Sv_{min} = f_A(r^*_{min})$ and for $Sv_{max} = f_A(r^*_{max})$, there are two solutions. For $f_A(r^*_{min}) < Sv < f_A(r^*_{max})$, there are three solutions.

~~The stability~~ Not only is the existence of the solutions important but their stability as well. Let $r_0$ denote an arbitrary solution of Eq. 6. The exact form of the stability condition of the solution ~~$r^*_0$~~ $r^*_0$ is governed by the function $\phi(r^*_0)$ (as defined in Marcu et al. (1995)). The ~~exact condition depends~~ condition can take two different forms depending on the sign of ~~$\phi(r^*_0)$. Since the~~ this function.

$$\phi(r^*_0) = \frac{1}{(2\pi)^2}\left[\frac{1-\exp(-r^{*2}_0/2)}{r^{*2}_0}\right]\left[\frac{1-\exp(-r^{*2}_0/2)}{r^{*2}_0} - \exp(-r^{*2}_0/2)\right] \tag{7}$$

The function has only one zero at ~~$r^*_s = 1.585201$, there are two cases~~ $r^*_s$ (see Table 3). For small radii ($r^*_0 < r^*_s$), the equilibrium is stable if:

$$\frac{St}{A} \leq \frac{1}{|\phi(r^*_0)|}\frac{1}{|\phi(r^*_0)|}. \tag{8}$$

For greater radii ($r^*_0 > r^*_s$), the condition for stability depends explicitly only on $A$:

$$A \geq \sqrt{\phi(r^*_0)}. \tag{9}$$

The equilibrium point satisfying the first type of the condition was shown to be a focus~~;~~, the second type ~~, a node. Different scenarios of particle motion determined by above stability conditions were shown in Fig.4 in Marcu et al. (1995). Fig. 4 here presents a simplified illustration of one of the scenarios: three equilibrium points, unstable point near the axis, stable point far from the axis, and droplets rotating around the vortex center.~~

~~Example illustration of droplet trajectories in 2D space (projection on a plane perpendicular to the vortex axis). Particle trajectories (color lines) show the presence of three equilibrium points marked with black dots: I - unstable near vortex axis, II - unstable middle distance point, III - stable point far from the axis. Some droplets rotate around the vortex core on various orbits, some of these orbits may correspond to limit cycles. Different attraction regions can be noticed.~~

**Table 4.** Stability conditions of particle equilibrium points present in the Burgers vortex with respect to vortex strain parameter $A$ and dimensionless distance from the vortex axis $r^*$. $A_t$, $\varphi(r^*)$, $r_s^*$, $r_{min}^*$ and $r_{max}^*$ defined in the text body.

| | $\leq r_s^*$ | $(r_s^*, r_{max}^*)$ | $[r_{max}^*, r_{min}^*)$ | $\geq r_{min}^*$ |
|---|---|---|---|---|
| $A < A_t$ | unstable for $St > A/\lvert\phi(r_0^*)\rvert$ | stable | partly unstable | stable |
| $A \geq A_t$ | | stable | | |

~~Particle motion along the vortex axis is separated from the motion 2D space and can be found analytically. It is determined by stretching outflow drag and gravity. As a consequence, as found in (Karpinska and Malinowski, 2014), position $z$ shows an exponential dependence on time. Every droplet has one unstable equilibrium point $z_0^* = SvA^{-1}\cot\theta$.~~

## 4 ~~Conditions for Void Creation~~

~~The results described above were used to formulate the following hypothesis concerning conditions of void creation: a majority of the polydisperse droplets in cloud must have an unstable equilibrium point close to the axis $r_0^* < r_s^*$ (leading to a limit cycle or periodic orbit). Attraction by a coexisting stable equilibrium point far from the axis $r_0^* > r_{min}^*$ should not influence their trajectories in a certain volume around the void.Hence, the analysis~~ to be a node.

Analysis of the equilibrium point stability conditions ~~has to be expanded by putting~~ by Marcu et al. (1995) is expanded here with emphasis on the dependence on strain parameter $A$. The results ~~were~~ are described in detail below and ~~are~~ summarised in Table 4.

~~The stability conditions change for $A_t = \max_{r_0^*}\left(\sqrt{\varphi(r_0^*)}\right) \approx 0.01917$. It is the maximum of right-hand side in Inequality 9 obtained numerically~~ Generally, stability conditions are different for $A$ ranges separated by $A_t = \max_{r_0^*}\left(\sqrt{\varphi(r_0^*)}\right)$ (approximate value obtained numerically in the Table 3). $A > A_t$ always satisfies then the condition expressed by 9. The term "partly unstable" in the table refers to the following: In the range of ~~$r_0^* \in [r_{max}^*, r_{min}^*)$~~ $r_{max}^* \leq r_0^* \leq r_{min}^*$, for a given $A$, only a small fraction of the total range (near points $r_{max}^*$ and $r_{min}^*$) is stable. This range grows with increasing $A$. Numerical experiments show, however, that their domain of attraction in the presence of other stable points (at least one exists always) is relatively small.

Combination of multiple existence conditions with stability conditions creates a variety of single particle motion scenarios. Some of them are shown in Fig.4 in Marcu et al. (1995). These scenarios are used in the next section to carry out a search for vortex model parameter values that produce a void. Fig. 4 here illustrates one of these scenarios in which there are three equilibrium points: I - unstable point near the axis, II - unstable middle distance point, III - stable point far from the axis. A particle, depending on initial position and velocity, rotates around point I or is weakly attracted by unstable point II or is strongly attracted by stable point III.

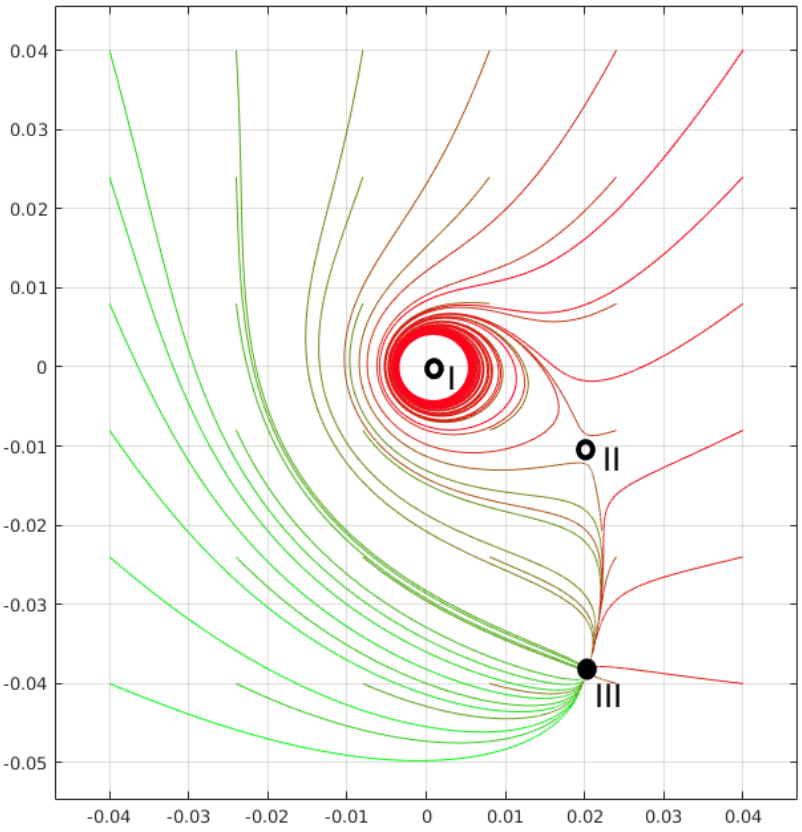


**Figure 4.** Example illustration of monodisperse droplets trajectories in 2D space (projection on a plane perpendicular to the vortex axis) with zero initial velocity. Particle trajectories (color lines) show the presence of three equilibrium points marked with black dots: I - unstable near vortex axis, II - unstable middle distance point, III - stable point far from the axis. Some droplets rotate around the vortex core on various orbits, some of these orbits may correspond to limit cycles. Different attraction regions can be noticed.

## 4 Cloud void creation conditions

Using conclusions concerning motion of a single particle, the following hypothesis on polydisperse particle collective behaviour can be formulated: a void can be created if a majority of the droplets have an unstable equilibrium point close to the axis $r_0^* < r_s^*$, leading to a limit cycle or periodic orbit attraction. Radius of curvature should be large enough for a void to be noticable. In case of multiple equillibrium points existence, attraction by stable equilibrium point far from the axis $r_0^* > r_{min}^*$ should not considerably influence droplet trajectories close to the void considerably. The first and the last condition are inspected in the first subsection below, the second condition in the next subsesction.

### 4.1 Polydisperse particles

Obtaining mathematically strict condition for creation of an arbitrary sized void in arbitrary polydisperse collection of droplets ~~is~~ would be too detailed and too complicated to be ~~used directly for comparison with~~ profitable for explanation of crude experimental results. Thorough analysis of single droplet motion ~~however, can be~~ in addition to what was presented in the paper (Marcu et al., 1995)) was performed and used to draw approximate conclusions ~~. The obvious statement~~ about polydisperse droplet motion.

The most obvious conclusion is that when circulation of the vortex is too small: $A \geq A_{cr}$, the motion of particles is determined mostly by the gravitational force and resembles ~~simple falling~~ sedimentation through the vortex ~~, but~~ with curved trajectories. ~~In the case~~ Circulation must then be large enough: at least $A \leq A_{cr}$ ~~Table 4 indicates that the void can be createdif the majority of particles have unstableequillibrium points near the center. Radial position of such a point $r^*$~~ for a void to be created.

The other condition is that equillibrium points near the vortex center for majority of the particles are unstable, allowing circulation around the vortex axis. Inequality 8 is exploited below to find the qualitative depenedence between vortex and particle parameters that fulfills this condition.

Firstly distance from the vortex axis of the equillibrium point should be in the range $r^* \leq r_s^*$ ~~can be approximated using a linearization of~~ . It allows approximation of relation described by Eq. 6 ~~:~~

in the vicinity of $r^* = 0$. The approximation is made with the assumption that in this vicinity the dependence on $A$ is weak (see Fig.2 in Marcu et al. (1995)).

$$\left(\frac{Sv}{A}\right)^2 = r^{*2}\left[1+\left(\frac{1-\exp\left(-r^{*2}/2\right)}{2\pi A r^{*2}}\right)^2\right] = r^{*2} + \frac{(1-\exp\left(-r^{*2}/2\right))^2}{(2\pi A r^*)^2} \simeq r^{*2} + \frac{1}{4\pi^2 A^2}\frac{r^{*2}}{4} = r^{*2}\left(1+(4\pi A)^{-2}\right), \tag{10}$$

so in the end:

$$r^* \simeq 4\pi S v \left(1+(4\pi A)^2\right)^{-\frac{1}{2}}. \tag{11}$$

~~The function determining stability condition (Eq. 8) can be approximated in this range as follows: $\phi(r_0^*) \simeq -(1-r_0^*/r_s^*) * (16\pi^2)^{-1}$~~ Sec the function $\phi(r_0^*)$ (see Fig.3 in Marcu et al. (1995)) is approximated in chosen $r^*$ range by linear dependence on $r^*$ :

$\phi(r_0^*) \simeq -(1 - r_0^*/r_s^*) \cdot (16\pi^2)^{-1}$. At $r^* = 0$ it has the same form as obtained for the case without gravity in Marcu et al. (1995). ~~Further stability analysis requires introducing a new dimnensionless parameter $B$:~~

$$B = \underbrace{\frac{r_s^*}{2^8\pi^3}}_{const} \frac{\nu^2}{g \sin\theta \delta^3}.$$

The above approximations are used in simplification of the stability condition determined by Eq. 8. In the end the condition for unstable points near the axis ~~splits in~~ are algebraicly transformed and expressed by spliting it in two parts. The first part concerns only the vortex parameters and the second part the particle sizes.

The first part requires that strain parameter $A$ ~~must be small enough~~(is small enough:

$$A < A_{max} \propto B^{1/3} \tag{12}$$

and consequently circulation ~~large enough):~~

$\Gamma$ large enough:

$$A < A_{max} = 2^{-1/6} B^{1/3} + O(\Gamma > \Gamma_{min} \propto B^2). \tag{13}$$

The second part demands that particle Stokes number falls within the range $(St_1, St_1 + \Delta St)$ and it is related to the vortex parameters (results shown to the leading term order in $A$):

$$\begin{aligned} St_1 &\propto A \\ \Delta St &\propto BA^{-2} \end{aligned} . \tag{14}$$

$B$ is a new dimnensionless parameter depending on vortex core size $\delta$ and gravity influence $gsin\theta$:

$$B = \underbrace{\frac{r_s^*}{2^8\pi^3}}_{const} \frac{\nu^2}{g \sin\theta \delta^3}. \tag{15}$$

Maximal strain parameter $A_{max}$ (minimal circulation $\Gamma_{min}$) increases (decreases) weakly with $B$. So the larger the vortex core size $\delta$ and gravity influence $gsin\theta$ the larger the minimal circulation needed.

The following ~~rough~~ conclusions can be drawn from the above approximated relations:

- There is a threshold (minimal) value of circulation needed for void creation. It increases with ~~gravity influence ($g \sin\theta$~~inclination angle ($\sin\theta$) and vortex size $\delta$.
- The greater the circulation the smaller particles have their unstable points near the axis.
- The range of particles having unstable points near the axis increases with increasing circulation and decreases with increasing gravity influence and vortex size $\delta$.

Building up on these results it may be concluded that it is harder to observe voids created by horizontally aligned vortices than vertically aligned ones and ~~the harder with increasing range of particle sizes~~it is the harder the larger particle size range is.

## 5 ~~Vortex Tube Model Parameter Ranges~~

### 4.1 Particle orbit in a void - radius of curvature

~~Using the above theoretical conclusions a careful search for vortex model parameter values was carried out to verify whether observed cloud voids could be attributed to the presence of vortex tubes. The search was made using simplified numerical simulations of droplet trajectories in vortices of varying circulation and orientation, and with dropletsof varying sizes. The results are described below~~In order to obtain a void, a majority of the droplets must circle around the axis and curvature of their trajectory should be large enough for a void to be noticable. In order to estimate the curvature radius we perform the following reasoning. For simplicity particle and vortex constants and parameters are now chosen to match those of water droplets in the cloudy air and henceforward particles are called droplets. Firstly, a basic vortex spatial scale is established for the measurement conditions. Premises found in the literature ~~described~~ discussed in the introduction were used for making the assumption that the proportionality constant in Eq. 1 is in the range $m \in [3.5, 24]$. ~~The relation between the vortex stretching parameter and the Kolmogorov length $\gamma = 2\nu\delta^{-2} = 2\nu(m\eta)^{-2}$ leads then to $\gamma \in [0.21, 8.35]s^{-1}$. Particle and vortex constants and parameters were chosen to match those of water droplets in the cloudy air and for the remaining discussion particles are called droplets. To estimate the range of the strain parameter, the following educated guess was made. void creation demands that most of the droplets in 2D space circle the vortex axis at a certain distance. Approximation of the~~ It means $\delta \in [0.18, 1.20]$ cm for August 27th measurements. Secondly, droplet trajectory curvature radius is approximated by the periodic orbit radius ~~described by~~ which is a solution of Eq. 5~~seems reasonable. Figure 5 presents contours of periodic orbit radius solutions as a function of vortex parameters. Contours were selected to match experimental void radii and are labeled in centimeters. Three droplet sizes$R$ were chosen to represent~~ . For this reason, various solutions of Eq. 5 are presented in Fig. 5 in function of vortex parameters. Every color represents one of droplet sizes: $R = 3, 13, 23\ \mu m$ chosen to be within the experimental range for August 27th (see Table 1). ~~Colored areas correspond to the periodic orbit existence condition ,~~ Overlapping colored surfaces match regions in which solutions can exist (what corresponds to the condition $St < St_{cr}$~~. This leads to the limitation of the strain parameter for further analysis to a range $A \in [5 \cdot 10^{-5}, 8 \cdot 10^{-3}]$. It can be noticed that $A < A_{cr}$, which according to the analysis in Sec.?? means it is outside the purely gravitational regime, with the possibility of particles having one unstable equilibrium point near the vortex axis and /or one stable equilibrium point far from the axis~~). Dashed lines are contour plots of solutions of chosen (close to experimental) void sizes: 0.5 cm, 1.5 cm, 3 cm. Using the information presented in this plot, the analysed strain parameter was further limited, from $A < A_{cr}$ down to $A \in [10^{-4}, 8 \cdot 10^{-3}]$.

## 5 Mie scattering influence on particle imaging

~~Contour plot of stable periodic 2D orbit radius for droplets of radii $R = 3, 13, 23\ \mu m$ covering the experimental range on August 27th. Selected ranges of vortex parameters: stretching $\gamma$ and strain $A$ are in x an y axes, respectively. Overlapping (blue on a top, then pink and green) colored surfaces match regions in which stable periodic 2D orbit exist for a given droplet radius. Dashed contours match experimental void radii labeled in cm. Black points represent parameters set for simulations as described in the next section.~~

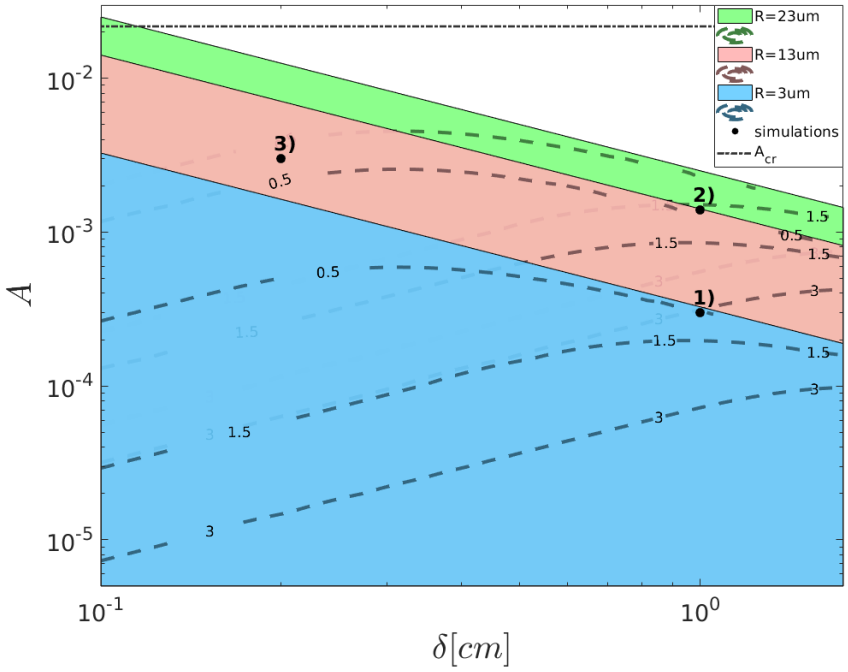


**Figure 5.** Contour plot of stable periodic 2D orbit radius for droplets of radii $R = 3, 13, 23\ \mu m$ covering the experimental range on August 27th. Selected ranges of vortex parameters: vortex core size $\delta$ and strain $A$ are in x an y axes, respectively. Overlapping (blue on a top, then pink and green) colored surfaces match subspaces in which stable periodic 2D orbit exist for droplet radius given by its colour. Dashed lines are contour plots of solutions of chosen void sizes:0.5 cm ,1.5 cm, 3 cm. Black points represent parameters set for simulations as described in the next section.

The Mie scattering theory is a rigorous mathematical theory describing the problem of elastic scattering of light by a dielectric sphere of arbitrary size and homogeneous refractive index in the case in which a sphere size is similar to or larger than the wavelength of the incident light. It shows a complex angular and particle size dependency of the scattered light intensity (van de Hulst, 1957). Thus brightness on images of laser light scattered by polydisperse set of droplets does not have to be monotonic with the droplet size. The reasons are described below.

Firstly the camera sensor pixel responds with a signal registration only if it receives an amount of energy exceeding a certain treshold. Light scattered on a particle passes through the optics and undergos some transformations. What is more particle image on the sensor is characterized by internal intensity distribution. Image size depends on particle size, optics magnification, position with respect to the focus and other factors (see Olsen and Adrian (2000)).

Secondly the scattered light intensity at an arbitrary angle depends nonlinearly on particle size. Bigger particle can give lower intensity than the smaller one or there may be several order of magnitude difference in intensity between particles differing by one order of magnitude in size.

For the purpose of our simplified analysis, the following assumptions are made:

- One particle image is recorded by one pixel,
- the signal received by a pixel changes linearly with incident light intensity only,
- particle is in focus and its image size and depends linearly on the particle size,
- the experiment in clouds was set up to allow best visualisation of maximal number of particles possible.

In order to compare results of the simulations with the measurements a procedure of droplet size and colour scaling is proposed. Mie scattering intensity calculation is performed with the help of algorithm that was described in Bohren and Huffman (2007). The scattering angle corresponds to 40 deg. In the size range of cloud particles the light intensity has a general growing tendency, but it is still strongly nonlinear. There are 3 orders of magnitude difference between particles of 1 $\mu$m and 30 $\mu$m radius. Relative intensity is calculated on this basis. Next, the brightness scaling is made. It assumes that experiment was set-up to let visualisation of 95% of particle size spectrum. Particle size at which particle size distribution cumulant reach 95% was calculated. Particles larger than this size have get brighness equal to 1 in the plots. The other particles brighness scales linearly with relative scattered light intensity. To mimic camera sensitivity there is a threshold below which particles get brighness 0. In the plot with white background the relation is opposite, so brightest particles are black, and the least bright are white. This color scaling was used in the next section for numerical simulation plots.

## 6 Numerical ~~Simulations~~Simulation Results

The hypothesis of cloud void appearance was verified by numerical simulations. To imitate processes occurring in real vortex tubes in clouds and examine the effect exerted on a droplet field by the presence of a vortex, a cylinder-shaped domain was chosen. At $t = 0$, the domain was filled uniformly with a given number concentration $n$ of droplets. Droplets leaving the

**Table 5.** Sets of vortex and particle parameters chosen for numerical simulation. $St$, $Sv$, $Fr$ are mean values. Only sets 1) and 2) give the visual effects of the cloud void.

| | ~~$\gamma\,[\frac{1}{s}]$~~ $\delta\ [cm]$ | $\theta$ | $A$ | $A_{max}$ | $\tau_f\,[s]$ | $St$ | $Sv$ | $Fr$ |
|---|---|---|---|---|---|---|---|---|
| 1) | ~~0.5~~ 1.0 | ~~0.78~~ $3\pi/8$ | ~~$\pi/8$~~ 0.0003 | ~~0.00036~~ 0.0017 | ~~0.003~~ 0.0020 | ~~1.45~~ 1.23 | ~~0.0014~~ 0.0034 | ~~31.82~~ 360 |
| 2) | ~~0.2 1.2~~ 1.0 | $\pi/4$ | ~~0.0048~~ 0.0014 | ~~0.0016~~ 0.0017 | ~~0.045~~ 0.0093 | ~~0.055~~ 0.26 | ~~0.91~~ 0.0159 | 17 |
| 3) | 0.5 | ~~0.78~~ $3\pi/8$ | ~~$\pi/4$~~ 0.0030 | ~~0.0076~~ 0.0030 | ~~0.0024~~ 0.0050 | ~~0.068~~ 0.49 | ~~0.057~~ 0.0223 | ~~1.096~~22 |

simulation domain were ~~constantly~~ removed, and no interaction between droplets was imposed. Initial positions of the new droplets ~~appearing in the domain~~ at $t > 0$ were randomized on the cylinder surface to obtain conditions "outside the cylinder" of homogeneous spatial distribution with the same $n$. The initial velocity of these droplets was adjusted to the radial inflow velocity. The simulation domain size was chosen to be capable of showing phenomena at scales larger than standard experimental cloud void size, such that $Z =$ ~~12~~ 20 cm long and $D = 5$ cm in radius. Sensitivity to different values of $D$ was examined, and no significant dependence on void creation was noticed. ~~An almost constant droplet number~~ Droplet trajectories were calculated by solving numerically Eq.3 in Burgers vortex velocity field. Droplet number concentration within the domain ~~was obtained in the course of the simulation. A semi-Gaussian distribution of droplet radii cut off at $R = 1.5\mu$m was chosen for simulations to match the experimental values~~ is almost constant and pattern does not change. Droplet radius distribution matches the experimental distribution from the 27th of August (see Table 1 and Fig.2 for comparison). Since droplets do not interact with each other and results do not depend on droplet concentration, $n = 10$~~cm$^{-3}$ or $n = 20$~~ cm$^{-3}$ was chosen ~~in order to minimize computational time. After 5 s to 8 s each simulation reached stationarity.~~

~~Experimental images of cloud voids were obtained with monochromatic green laser light scattered by spherical droplets at a certain forward angle (see Sec. 2). A large variability in visibility of individual droplets marginally differing in radius could, due to Mie scattering properties, influence observed patterns resulting from voids. To reflect these effects~~ as a compromise between computational costs and visibility purposes. After a few seconds each simulation becomes steady. 40° scattering angle was chosen for calculation of Mie effect in the post-processing of simulation results~~, a 40° scattering angle was used. Visualizations in Fig.5 show droplets scaled by both size and color brightness in order to represent scattered light intensity. The Mie scattering algorithm used is described in (Raffel et al., 1998)~~.

~~Two simulations~~Three simulations' parameter sets are presented below. Two of them, 1) and 2) ~~, with parameters described~~ in Table 5 may result in the presence of a round or close to round void around the vortex axis. Simulation 3) does not show anything close to void creation or any other persistent pattern formation. ~~The three simulation cases were chosen to indicate that the theoretical prediction presented in Fig.5 is just an approximate tool to manage a complex problem.: although parameter sets 2) and 3) are on the "no-void" side, case 2 gives visible impression of a void. This is further confirmed by noticing that value of $A$ in case 2) is greater than $A_{max}$. It means that even in the case of droplets being attracted by their stable points near the axis it is possible that the attraction is weak. Just a few seconds of motion resembles rotation around an unstable point which is able to create a void.~~

Figure 6 presents a 3D ~~picture~~ views (panels a and b) with a 2D ~~cross-section~~ cross-sections (c and d) at the last, quasi stationary stage of simulations 1) and 2). In the database (Karpinska et al., 2018) one may find 2D and 3D animations from the simulations~~both in 2D and 3D~~. Animations "ms03" and "ms04" correspond to set 1), "ms05" and "ms06" to set 2), "ms07" and "ms08" to set 3).

~~To qualitatively present the droplet spatial structure in a void, all droplets were~~ Droplet spatial distribution in and around presented voids show signs of clustering and segregation. Standard quantitative indicators of these phenomena (radial distribution function, fractal dimension, Voronoi diagram, segregation lenght) designed for homogeneous isotropic turbulence in our case would be difficult to interpret so another approach is proposed.

Droplet size distribution was divided into five bins in a way the bins are equal in droplet number. Number concentration $n$ with respect to the distance from the vortex axis $r$ was plotted in panels e~~and f~~) and f) of Fig. 6~~with different shading colors representing~~. The ploted $n$ values represent the mean over 50 succesive time instants. Different shading colors represent contributions from different size groups~~. A homogeneous~~, so the darkest plot represents smallest droplets - first size group, the brighter represents the first and the second size group together etc. If the distribution of droplets in ~~space would give a horizontalline. Sorting and clustering effects of the vortex presence caused by attraction of stable equilibrium points and limit cycles are clearly seen. Line~~ the domain was homogeneous it would be plotted as horizontal, parallel, equally spaced lines. Red line plots in the same panel present droplet mean radius $\langle R \rangle$ and droplet mean visible radius $\langle S \rangle$ ~~(scaled according to Mie scattering) with respect to the distance from vortex axis $r$~~versus distance from the vortex axis. Visible radius reflects droplet relative sizes in the camera image estimated by including Mie scattering and the camera threshold sensitivity influence as defined in Sec.5. In the absence of sorting ~~and clustering, the~~ both plots would approach ~~horizontal lines.Their actual shape demonstrates a strong influence of droplet sorting on strengthening the visible void effect. On the basis of the real droplet radius plot, the radii of the voids can be estimated as $\sim$ 0-1.5 cm; however, the visible~~ one horizontal line.

Panels e and f of Fig. 6 show that droplets around the void ~~radii are rather $\sim$ 2-2.5 cm, which seems close to the experimental values and is on the order of the Burgers vortex core size $\delta$~~are nonhomogeneously distributed and segregated by size in space. The most inner part of the figure in panel e) is almost devoid of droplets. The larger distance from the axis the bigger the particles circling around the void. Animations of motion clearly present that this is caused by limit cycle attraction, which radius apparently grows with droplet size. This is pronounced in panel c as well. Visible void radius is around 2.5 cm, whereas "real" (no droplets) void radius is estimated to be 1 cm. Panel f of Fig. 6 shows more blurry situation: the inner part of the vortex is not empty, but the droplets are smaller (less visible) then those more away from the axis. For increasing visibility treshold visible void size increase in both cases.

Values of $St$, $Sv$ (mean of polydisperse particle set) in simulated vortices differ essentialy from values in Table 1. Estimations of $St$ and $Sv$ in 3D real turbulence flow are based on a global value - Kolmogorov timescale. Calculation in the simulation use vortex model characteristic times. Local parameter values of single vortex in intermittent turbulent flow can be completely different then global flow characteristics.

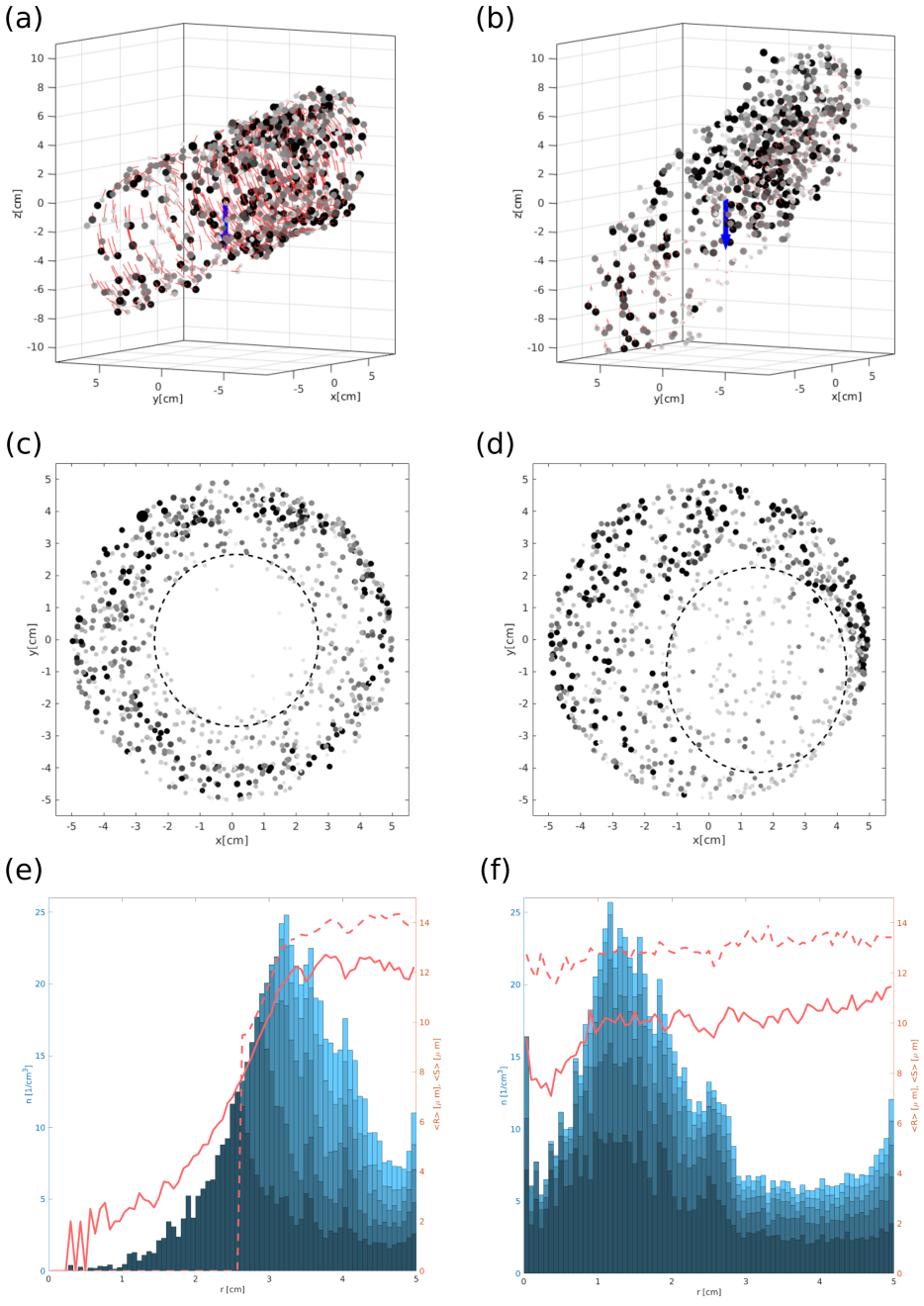


**Figure 6.** Positions of droplets in simulations 1) (left side) and 2) (right side) as described in Table 5 in perspective view (panels a and b) and in ~~2 cm~~4 *cm*-thick central slice projected on a plane perpendicular to the vortex axis (panels c and d). The blue arrow shows the direction of gravity. In panels a-d, droplet ~~color and~~ size and colour are ~~proportional~~ scaled respectively to the ~~Mie scattering intensity~~rules described in Sec.5. The red ~~lines~~ tracks behind the particles in panels a and b reflect the last ~~$\Delta t = 0.06$ s~~ $\Delta t = 0.0055$ s of the droplet trajectory (for clarity every 10th droplet is drawn). The ~~gray~~ dashed circles in panels c and d reflect the approximate shape and size of the visible void in the droplet field. Panels e ~~)~~ and f ~~)~~ present: the number concentration of droplets $n$ with different blue shading colors representing the contribution from different size groups - left axis, droplet mean real radius (solid red line) ~~; right axis~~ and mean visible radius (dashed red line) - right axis, all with respect to the distance from the vortex axis $r$.

In summary, there are two possible factors together creating the visible effect of the void. The first one is collective droplet dynamics: the majority of the droplets move on helical trajectories, being attracted in 2D space by the limit cycle or by a stable point near the axis. ~~The largest ones~~ Large droplets may be slowly attracted by their equilibrium point far from the vortex axis in 2D space, but in the course of attraction they circle around the axis. At the same time, a significant ratio of the characteristic timescale of motion in the plane perpendicular to vortex axis with respect to motion along the vortex axis is needed. ~~The second factor is the visibility of droplets in the laser sheet: variation of Mie scattering intensities with droplet radius is large, so the smallest droplets moving towards their stable equilibrium point near~~ Secondly, segregation of particles with respect to the distance from the vortex axis can influence visible void size due to Mie scattering effects. Even if the circulation is not strong enough to displace the smallest particles far from the vortex axis ~~may not be visible in the laser sheet picture. This strengthens visible void creation for $A > A_{max}$ as in the simulation set 2). In effect, there may exist a wide range of vortex parameters that can result in the visual effect of a void of a certain radius for a given droplet size distribution.~~it is possible that their images are not recorded by the camera. Therefore visible void size can depend vitally on imaging capability.

## 7 Discussion and Conclusions

Visualizations of cloud droplets by means of laser sheet photography performed at the Schneefernerhaus observatory revealed the presence of voids - holes in the form of curved elongated cylinders with a radius of a few centimeters~~(see the movie in the supplementary materials)~~. The possibility of such cloud voids or “Swiss cheese" cuts in clouds was suggested by former studies of the Stokes motion of cloud droplets in idealized Burgers or line vortices. Using information on cloud droplet size distributions and turbulence parameters collected in the course of observations, as well as literature discussions on vortex tubes in turbulent flows, we have shown that the cloud voids observed under the experimental conditions were ~~very~~ likely a result of the presence of relatively thin yet long vortex tubes. Approximate theoretical conditions of void creation ~~on primarily vortex tube circulation and other vortex and droplet parameters were proposed~~ were proposed and vortex circulation was shown to be the parameter of the greatest importance in the conditions formulation. The calculations are consistent with the observation that voids are present under some conditions and not under others. Comparison of the modeled and ~~observed~~ experimental voids led to the conclusion that properties of the Mie scattering ~~of laser sheet light have to be accounted for to reproduce~~ play great role in reproducing of the proper size and shape of ~~the observed cloud voids~~ cloud voids observed by laser imaging.

This finding, if confirmed in clouds far from the atmospheric surface layer, might help to better understand the effect of high Reynolds number turbulence on clustering, size ~~sorting~~ segregation and probably collisions of cloud droplets. In the literature, several perspectives on ~~this problem were presented: the centrifuge mechanism for small St particles in the dissipation range in Maxey (1987); the sweep-stick mechanism described in Coleman and Vassilicos (2009) correlating fluid zero-acceleration points with droplet clusters; caustics - points in space of multiple valued particle velocity, as summed up in Gustavsson and Mehlig (2016) - or the sling effect, analogous to caustics, presented in Falkovich and Pumir (2007). Considering~~ the clustering mechanism were presented, to name just a few: Maxey (1987), Coleman and Vassilicos (2009), Falkovich and Pumir (2007),Gustavsson and Mehlig (2011).

The paper of Gustavsson and Mehlig (2016) presents a thorough review of research on clustering. Authors are aware of the fact that considering droplet motion within a single vortex ~~,~~as a representative of coherent dissipative structures expected to exist in turbulent flows, ~~as in the present paper,~~ is a strong simplification in comparison to the cited works. However, the research conducted for non-sedimenting particles in Ravichandran and Govindarajan (2015), Deepu et al. (2017) suggests that fixed point attraction and caustics formed by limit cycle attraction strongly increase the clustering and collisions of particles near single and multiple vortices. This fact should become very distinct motivation for investing in both experimental and theoretical research aiming at thorough quantitative characterization of cloud void events.

*Code and data availability.* Numerical simulation code available on demand. Data repository containing experimental movies and animations of simulations is retrieved from: https://www.researchgate.net/publication/328429794_Data_supporting_the_paper_Turbulence_induced_cloud_voids_observation_and_interpretation.

*Author contributions.* Raymond Shaw, Holger Siebert and Eberhard Bodenschatz designed the experiment. Szymon Malinowski formulated the aim for theoretical and numerical analysis. Steffen Risius, Tina Shmeissner, Raymond Shaw, Holger Siebert, Hengdong Xi, Haitao Xu Jonathan Bodenschatz and Eberhard Bodenschatz provided resources and carried out the experiment. Tina Shmeissner, Steffen Risius, Haitao Xu, Eberhard Bodenshatz maintained and synthesized experimental data. Szymon Malinowski and Eberhard Bodenschatz acquired financial support. Katarzyna Karpińska and Szymon Malinowski developed numerical model. Katarzyna Karpińska analysed the experimental data, conducted theoretical analysis, designed and implemented the code for numerical analysis, conducted validation and verification of numerical results, wrote the original draft of the paper. Katarzyna Karpińska and Steffen Riusius provided visualisation of the results. Szymon Malinowski was responsible for supervision. Katarzyna Karpinska, Szymon Malinowski, Jakub Nowak, Steffen Riusius, Raymond Shaw and Holger Siebert edited the original draft to prepare it for submission.

*Competing interests.* No competing interest are present.

*Acknowledgements.* We are grateful to Mr. Markus Neumann and the staff at UFS for their technical help at UFS and the Bavarian Umweltministerium for the financial support of the station. Financial support from Max Planck Society, Deutsche Forschungsgemeinschaft (DFG) through the SPP 1276 Metström, the EU COST Action MP0806 Particles in Turbulence, Polish National Science Centre (grant 2013/08/A/ST10/00291) and through the US National Science Foundation (NSF grant AGS-1026123) are gratefully acknowledged. We thank Marta Wacławczyk and Liang Ping Wang for the comments on the manuscript.

## References


Belin, F., Moisy, F., Tabeling, P., and Willaime, H.: Worms in a turbulence experiment, from hot wire time series, in: Fundamental Problematic Issues in Turbulence, Trends in Mathematics, p. 129–140, 1999.

Biferale, L., Scagliarini, A., and Toschi, F.: On the measurement of vortex filament lifetime statistics in turbulence, Physics Letters A, 276, 115–121, 2000.

Bodenschatz, E., Malinowski, S. P., Shaw, R. A., and Stratmann, F.: Can We Understand Clouds Without Turbulence?, Science, 327, 970–971, https://doi.org/10.1126/science.1185138, http://science.sciencemag.org/content/327/5968/970, 2010.

Bohren, C. F. and Huffman, D. R.: Absorption and Scattering of Light by Small Particles, 2007.

Burgers, J.: A Mathematical Model Illustrating the Theory of Turbulence, vol. 1 of *Advances in Applied Mechanics*, p. 171–199, Elsevier, https://doi.org/10.1016/S0065-2156(08)70100-5, http://www.sciencedirect.com/science/article/pii/S0065215608701005, 1948.

Calzavarini, E., Cencini, M., Lohse, D., and Toschi, F.: Quantifying Turbulence-Induced Segregation of Inertial Particles, Phys. Rev. Lett., 101, 084 504, https://doi.org/10.1103/PhysRevLett.101.084504, https://link.aps.org/doi/10.1103/PhysRevLett.101.084504, 2008.

Chuang, P. Y., Saw, E. W., Small, J. D., Shaw, R. A., Sipperley, C. M., Payne, G. A., and Bachalo, W. D.: Airborne Phase Doppler Interferometry for Cloud Microphysical Measurements, Aerosol Science and Technology, 42, 685–703, https://doi.org/10.1080/02786820802232956, http://dx.doi.org/10.1080/02786820802232956, 2008.

Coleman, S. W. and Vassilicos, J. C.: A unified sweep-stick mechanism to explain particle clustering in two- and three-dimensional homogeneous, isotropic turbulence, Physics of Fluids, 21, 113 301, https://doi.org/10.1063/1.3257638, https://doi.org/10.1063/1.3257638, 2009.

Deepu, P., Ravichandran, S., and Govindarajan, R.: Caustics-induced coalescence of small droplets near a vortex, Physical Reviev Fluids, 2, 024 305, https://doi.org/10.1103/PhysRevFluids.2.024305, https://link.aps.org/doi/10.1103/PhysRevFluids.2.024305, 2017.

Falkovich, G. and Pumir, A.: Sling Effect in Collisions of Water Droplets in Turbulent Clouds, Journal of the Atmospheric Sciences, 64, 4497–4505, https://doi.org/10.1175/2007JAS2371.1, 2007.

Gerber, H., Frick, G., Malinowski, S. P., Brenguier, J.-L., and Burnet, F.: Holes and Entrainment in Stratocumulus, Journal of the Atmospheric Sciences, 62, 443–459, https://doi.org/10.1175/JAS-3399.1, https://doi.org/10.1175/JAS-3399.1, 2005.

Gustavsson, K. and Mehlig, B.: Ergodic and non-ergodic clustering of inertial particles, EPL (Europhysics Letters), 96, 60 012, https://doi.org/10.1209/0295-5075/96/60012, https://doi.org/10.1209%2F0295-5075%2F96%2F60012, 2011.

Gustavsson, K. and Mehlig, B.: Statistical models for spatial patterns of heavy particles in turbulence, Advances in Physics, 65, 1–57, 2016.

Hill, R. J.: Geometric collision rates and trajectories of cloud droplets falling into a Burgers vortex, Physics of Fluids, 17, 037 103, https://doi.org/10.1063/1.1858191, 2005.

Jimenez, J. and Wray, A.: On the characteristics of vortex filaments in isotropic turbulence, Journal of Fluid Mechanics, 373, 255–285, 1998.

Jiménez, J., Wray, A., Rogallo, R., and Saffman, P.: The structure of intense vorticity in isotropic turbulence, Journal of Fluid Mechanics, 255, 65–90, 1993.

Karpinska, K. and Malinowski, S.: Towards better understanding of preferential concentration in clouds: droplets in small vortices, in: American Meteorological Society 14th Conference on Cloud Physics, 2014.

Karpinska, K., Bodenschatz, J. F., Malinowski, S. P., Nowak, J. L., Risius, S., Schmeissner, T., A.Shaw, R., Siebert, H., Xi, H., Xu, H., and Bodenschatz, E.: Data supporting the paper "Turbulence induced cloud voids: observation and interpretation"., 2018.

Marcu, B., Meiburg, E., and Newton, P. K.: Dynamics of heavy particles in a burgers vortex, Physics of Fluids, 7, 400–410, 1995.

Markowicz, K., Bajer, K., and Malinowski, S. P.: Influence of small-scale turbulence structures on the concentration of cloud droplets, in: 13th Conference on Clouds and Precipitation, IAMAP, 2000.

Maxey, M. R.: The gravitational settling of aerosol particles in homogeneous turbulence and random flow fields, Journal of Fluid Mechanics, 174, 441–465, https://doi.org/10.1017/S0022112087000193, 1987.

Maxey, M. R. and Corrsin, S.: Gravitational Settling of Aerosol Particles in Randomly Oriented Cellular Flow Fields, Journal of the Atmospheric Sciences, 43, 1112–1134, https://doi.org/10.1175/1520-0469(1986)043<1112:GSOAPI>2.0.CO;2, 1986.

Moisy, F. and Jimenez, J.: Geometry and clustering of intense structures in isotropic turbulence, Journal of Fluid Mechanics, 513, 111–133, https://doi.org/10.1017/S0022112004009802, 2004.

Mouri, H., Hori, A., and Kawashima, Y.: Vortex tubes in velocity fields of laboratory isotropic turbulence, Physics Letters A, 276, 115–121, 2000.

Neu, J. C.: The dynamics of stretched vortices, Journal of Fluid Mechanics, 143, 253–276, https://doi.org/10.1017/S0022112084001348, https://www.cambridge.org/core/article/dynamics-of-stretched-vortices/1783CBAF5D397FD30CD90BB137533477, 1984.

Olsen, M. G. and Adrian, R. J.: Out-of-focus effects on particle image visibility and correlation in microscopic particle image velocimetry, Experiments in Fluids, 29, S166–S174, https://doi.org/10.1007/s003480070018, https://doi.org/10.1007/s003480070018, 2000.

Pirozzoli, S.: On the velocity and dissipation signature of vortex tubes in isotropic turbulence, Physica D Nonlinear Phenomena, 241, 202–207, 2012.

Raffel, M., Willert, C., and Kompenhans, J.: Particle Image Velocimetry: A Practical Guide, Engineering online library, Springer Berlin Heidelberg, https://books.google.pl/books?id=dopRAAAAMAAJ, 1998.

Ravichandran, S. and Govindarajan, R.: Caustics and clustering in the vicinity of a vortex, Physics of Fluids, 27, 033 305, https://doi.org/10.1063/1.4916583, https://doi.org/10.1063/1.4916583, 2015.

Risius, S., Xu, H., Di Lorenzo, F., Xi, H., Siebert, H., Shaw, R. A., and Bodenschatz, E.: Schneefernerhaus as a mountain research station for clouds and turbulence, Atmospheric Measurement Techniques, 8, 3209–3218, https://doi.org/10.5194/amt-8-3209-2015, http://www.atmos-meas-tech.net/8/3209/2015, 2015.

Shaw, R. A.: Supersaturation Intermittency in Turbulent Clouds, Journal of the Atmospheric Sciences, 57, 3452–3456, https://doi.org/10.1175/1520-0469(2000)057<3452:SIITC>2.0.CO;2, 2000.

Shaw, R. A., Reade, W. C., Collins, L. R., and Verlinde, J.: Preferential Concentration of Cloud Droplets by Turbulence: Effects on the Early Evolution of Cumulus Cloud Droplet Spectra, Journal of the Atmospheric Sciences, 55, 1965–1976, https://doi.org/10.1175/1520-0469(1998)055<1965:PCOCDB>2.0.CO;2, 1998.

Siebert, H., Shaw, R. A., Ditas, J., Schmeissner, T., Malinowski, S. P., Bodenschatz, E., and Xu, H.: High-resolution measurement of cloud microphysics and turbulence at a mountaintop station, Atmospheric Measurement Techniques, 8, 3219–3228, https://doi.org/10.5194/amt-8-3219-2015, http://www.atmos-meas-tech.net/8/3219/2015, 2015.

Tanahashi, M., Fujibayashi, K., and Miyauchi, T.: Fine Scale Eddy Cluster and Energy Cascade in Homogeneous Isotropic Turbulence, Proceedeings of IUTAM Symposium on Computational Physics and New Perspectives in Turbulence, 4, 67–72, 2008.

Tennekes, H. and Woods, J. D.: Coalescence in a weakly turbulent cloud, Quarterly Journal of the Royal Meteorological Society, 99, 758–763, https://doi.org/10.1002/qj.49709942215, http://dx.doi.org/10.1002/qj.49709942215, 1973.

van de Hulst, H. C.: Light scattering by small particles, p. 470; 103, https://doi.org/10.1002/qj.49708436025, https://rmets.onlinelibrary.wiley.com/doi/abs/10.1002/qj.49708436025, 1957.

Warhaft, Z.: Passive Scalars in Turbulent Flows, Annual Review of Fluid Mechanics, 32, 203–240, https://doi.org/10.1146/annurev.fluid.32.1.203, https://doi.org/10.1146/annurev.fluid.32.1.203, 2000.